LUPUS SCIENCE & MEDICINE™

RNA tape sampling in cutaneous lupus erythematosus discriminates affected from unaffected and healthy volunteer skin

Joseph F Merola,[1,2] Wenting Wang,[3] Carrie G Wager,[3] Stefan Hamann,[3] Xueli Zhang,[3] Alice Thai,[3] Christopher Roberts,[3] Christina Lam,[4] Cristina Musselli,[3] Galina Marsh,[3] Dania Rabah,[3] Catherine Barbey,[5] Nathalie Franchimont,[3] Taylor L Reynolds [3]

To cite: Merola JF, Wang W, Wager CG, *et al*. RNA tape sampling in cutaneous lupus erythematosus discriminates affected from unaffected and healthy volunteer skin. *Lupus Science & Medicine* 2021;**8**:e000428. doi:10.1136/lupus-2020-000428

► Additional material is published online only. To view, please visit the journal online (http://dx.doi.org/10.1136/lupus-2020-000428).

NF and TLR are joint senior authors.

Received 10 July 2020
Revised 20 December 2020
Accepted 17 January 2021

For numbered affiliations see end of article.

Correspondence to
Dr Taylor L Reynolds;
taylor.reynolds@biogen.com

ABSTRACT

Objective Punch biopsy, a standard diagnostic procedure for patients with cutaneous lupus erythematosus (CLE) carries an infection risk, is invasive, uncomfortable and potentially scarring, and impedes patient recruitment in clinical trials. Non-invasive tape sampling is an alternative that could enable serial evaluation of specific lesions. This cross-sectional pilot research study evaluated the use of a non-invasive adhesive tape device to collect messenger RNA (mRNA) from the skin surface of participants with CLE and healthy volunteers (HVs) and investigated its feasibility to detect biologically meaningful differences between samples collected from participants with CLE and samples from HVs.

Methods Affected and unaffected skin tape samples and simultaneous punch biopsies were collected from 10 participants with CLE. Unaffected skin tape and punch biopsies were collected from 10 HVs. Paired samples were tested using quantitative PCR for a candidate immune gene panel and semi-quantitative immunohistochemistry for hallmark CLE proteins.

Results mRNA collected using the tape device was of sufficient quality for amplification of 94 candidate immune genes. Among these, we found an interferon (IFN)-dominant gene cluster that differentiated CLE-affected from HV (23-fold change; p<0.001) and CLE-unaffected skin (sevenfold change; p=0.002), respectively. We found a CLE-associated gene cluster that differentiated CLE-affected from HV (fourfold change; p=0.005) and CLE-unaffected skin (fourfold change; p=0.012), respectively. Spearman's correlation between per cent area myxovirus 1 protein immunoreactivity and IFN-dominant mRNA gene cluster expression was highly significant (dermis, rho=0.86, p<0.001). In total, skin tape-derived RNA expression comprising both IFN-dominant and CLE-associated gene clusters correlated with per cent area immunoreactivity of some hallmark CLE-associated proteins in punch biopsies from the same lesions.

Conclusions A non-invasive tape RNA collection technique is a potential tool for repeated skin biomarker measures throughout a clinical trial.

Key messages

What is already known about this subject?

- Interferon-responsive gene expression has been associated with cutaneous lupus erythematosus (CLE) pathogenesis and can be measured in skin biopsies; however, biopsy is relatively invasive and can result in infection or scarring.
- Skin tape RNA sampling is an emerging modality to potentially replace invasive skin biopsy; this technique has proven useful to inform on disease-specific gene expression in atopic dermatitis and psoriasis diseases and is in use in the clinic to diagnose melanoma.

What does this study add?

- To our knowledge, this is the first use of a non-invasive skin tape method to measure RNA expression in CLE skin.
- This study is also the first to identify gene signatures that discriminate between CLE-affected and healthy volunteers' skin and between CLE-affected and CLE-unaffected skin from tape-derived RNA.

How might this impact on clinical practice or future developments?

- This tape RNA method and associated gene signatures may be used as surrogate to punch biopsy to further elucidate CLE natural disease course and/or response to treatment. This novel use of the tape RNA technique will promote easier access to molecular data from CLE skin samples while prioritising patient welfare. While confirmation and validation of this methodology in a large-scale study is needed, it shows promise for use in precision medicine—the right treatment for the right patient.

INTRODUCTION

Cutaneous lupus erythematosus (CLE) is a chronic autoimmune disease that may present with or without SLE, and can be divided into acute, subacute and chronic CLE subtypes (including discoid lupus erythematosus [DLE] as a major subtype).[1 2] Although the pathogenesis of SLE and CLE are not fully elucidated, genetic risk, environmental

triggers and abnormalities in the innate and adaptive immune response have been implicated.[3 4]

Genetic and clinical observations have highlighted an essential role of type I, type II and type III interferons (IFN-I, IFN-II and IFN-III) in SLE and CLE pathogenesis.[5–13] A 'type I IFN signature' has emerged as a major risk factor for SLE disease activity.[5 14–17] IFN signatures, and myxovirus resistance protein A (MXA), a protein induced by IFN, have been detected in the affected skin of patients with active CLE.[18–20] The central role of IFN-I in CLE pathogenesis is further supported by data showing improvement in disease activity in participants with SLE with active skin disease treated with agents targeting IFN-I (anti-IFN-α or anti-IFN-I α/β receptor).[21–23] Recently, a humanised monoclonal antibody (BIIB059) targeting blood dendritic cell antigen 2 (BDCA-2), uniquely expressed on plasmacytoid dendritic cells (pDCs)—master regulators of the IFN response— showed following treatment a strong association between reduction in MXA expression in skin and reduction in disease activity and demonstrated efficacy in reducing disease activity in CLE.[20 24 25]

CLE diagnosis and follow-up is often supported by histological examination requiring a punch biopsy.[26] Disadvantages with punch biopsy include pain, localised bleeding, infection and potential scarring.[27] Consequently, this technique may impede patient recruitment into clinical trials and decrease patient compliance for follow-up visits. Development of a non-invasive technique for CLE biomarker assessment would offer a significant advantage for patient well-being while permitting monitoring of lesions over time.

Adhesive tape sampling is a non-invasive method that allows recovery of cells comprising and associated with the epidermal stratum corneum and granulosum.[28–34] Studies in atopic dermatitis (AD), contact dermatitis, psoriasis and melanoma have used non-invasive tape sampling to investigate disease-specific gene profiles and identify genomic tumour phenotypes and disease-associated transcriptomic endotypes.[28 29 33–37] Despite the basal epidermal, junctional and dermal anatomic locations of morphological changes in subacute cutaneous lupus erythematosus (SCLE) and DLE, as keratinocytes express increased levels of IFN-I and IFN-III genes and IFN-inducible genes within CLE lesions[13 19 38 39] and local IFN may invoke a hypersensitive response in lupus keratinocytes,[40] we hypothesised that expression of specific gene signatures in the epidermis would be detected at the site of skin lesions, and perhaps also in non-adjacent unaffected skin in participants with CLE.

This pilot research study assessed whether an adhesive tape device (https://dermtech.com), which is used in clinical practice for melanoma diagnosis, can recover informative RNA signals that would be specific of lupus disease pathogenesis from the epidermis of participants with DLE or SCLE, as compared and contrasted with healthy volunteers (HVs), and whether it can be used to identify a gene signature that may differentiate affected (A) from unaffected (U) skin. To compare RNA tape gene signature results with a traditional sampling method, from each skin lesion, paired tape RNA and punch biopsy samples were taken. Using punch biopsies, protein immunoreactivity from semi-quantitative immunohistochemistry (IHC) was correlated with gene signature scores from tape RNA.

MATERIALS AND METHODS

Study design

This cross-sectional cohort study was performed at two US study sites. Day 1 assessments included the collection of participants' characteristics, medical history and a photograph of the taping site for all participants. All participants underwent blood sampling and skin tape harvesting and, for participants who consented, an optional skin biopsy on day 1 (online supplemental figure S1); participants with DLE and SCLE also received a skin examination and disease activity assessment.

Study assessments

Disease activity for participants with DLE or SCLE was evaluated using Cutaneous Lupus Erythematosus Disease Area and Severity Index (CLASI)[41] and a Physician Global Assessment. Procedure-related adverse events (AEs) and serious AEs were monitored and recorded.

Study population

Included participants were aged ≥18 years at the time of informed consent. Participants had to present with active DLE or SCLE skin disease (with or without systemic manifestations of SLE).[42 43] Concomitant antimalarial or systemic immunosuppressive therapies were allowed if doses were stable for ≥28 days before the day 1 visit. Prednisone or equivalent maximum dosage was 15 mg/day. High-potency topical steroids and/or other topical agents had to be stopped 7 days before the day 1 visit. HVs had to be in good overall health as determined by the investigator. For further details, see inclusion and exclusion criteria in online supplementary materials.

Biomarker samples

Whole blood and punch biopsy samples were collected from 23 HVs, 9 participants with DLE (1 participant did not consent to a whole blood sample and 1 participant did not consent to a punch biopsy sample) and 1 participant with SCLE. Skin tape samples and punch biopsies were collected from participants with CLE-affected skin (CLE-A) and from HVs; only skin tape samples were collected from CLE-unaffected skin (CLE-U). Further details are in online supplementary materials.

RNA extraction and quantification of gene expression

RNA was extracted from tape using DermTech (La Jolla, California, USA; https://dermtech.com) protocols. Gene expression was quantified by quantitative PCR (qPCR) on the OpenArray platform (Thermo Fisher Scientific, Waltham, Massachusetts, USA). Further details regarding

sample quality and gene panels assessments (online supplemental tables S1 and S2) are in online supplementary materials.

Immunohistochemistry and image analysis

IHC for MXA, CD45 and CD303 was conducted on formalin-fixed, paraffin-embedded punch biopsies (online supplemental table S3). Immunoreactive areas were computed using custom-designed algorithms in Visiopharm (Hoersholm, Denmark) software. More details are in online supplementary materials.

Statistical analysis

Descriptive statistics were calculated for demographics and disease characteristics for each group. Individual tape samples were plotted on the first two principal components of log2 expression for all candidate genes. Using the gene expression data generated in the final analysis, candidate genes were grouped into four gene clusters based on the hierarchical clustering of the consensus of 1000 K-means results, after bootstrapping 80% of samples at each iteration (ConsensusClusterPlus R package). Using pooled data generated from interim analyses and final analyses, gene set scores and differences in gene set scores among disease groups were estimated using a linear mixed-effects model, with fixed effects for sample type and random intercepts for genes and samples. P values from multiple comparisons were adjusted using Tukey's correction. Spearman's correlations and associated p values were calculated to determine the associations between biomarkers from skin tape-derived RNA and IHC based on skin biopsies.

Additional details regarding statistical methods used for the gene expression analyses are included in the supplementary materials.

Computational biology analysis

Distinct gene clusters from K-means analysis were analysed for biological pathway enrichment using Ingenuity Pathways Analysis (Qiagen, Hamburg, Germany). Pathway enrichment p values were adjusted for multiple hypothesis testing.

Patient and public involvement

No patients or members of the public were involved in the design, or conduct, or reporting, or dissemination plans of this research.

RESULTS

Participant characteristics and safety

This cross-sectional study enrolled 23 HVs. Of these, 10 HVs were age-matched to participants with skin disease and included in the current analysis with 9 participants with active DLE and 1 participant with SCLE; baseline characteristics are presented in table 1. The mean ages for the study groups ranged from 55.7 to 58.0 years. The majority were female in the CLE group. Most participants in the HV, DLE and SCLE groups were white. Three participants with DLE had a concomitant SLE diagnosis. Relevant concomitant medication use was documented. Participants with CLE presented with mild to moderate skin disease activity; CLASI activity score[41] ranged from 4 to 19 and Physician Global Assessment score was between 10 and 30. Biopsy sites are shown in online supplemental table S4; for biopsy morphological descriptions, see online supplemental table S5.

One participant with DLE experienced two procedure-related AEs: itching at the site of biopsy and minor bleeding at the site of biopsy; both were mild in severity and resolved by day 2. No serious AEs or other AEs were reported during the study.

Tape-derived gene expression

Total RNA yields, pooled from 4 tapes per skin site, for 30 tape RNA samples averaged 42.58 ng (SD, 142.50 ng). No tape samples were removed from analysis based on low RNA yield. Gene expression was measured by qPCR amplification of 102 candidate genes. Eight genes were excluded from statistical analysis because the results did not meet quality control cut-off criteria (see online supplemental table S6 for a list of genes removed), resulting in expression analysis of 94 genes. Additional details are available in the supplementary materials.

To visualise a summary of gene expression of a panel of 94 candidate immune genes (online supplemental table S7) for each participant, we plotted tape-derived gene expression along the first two principal components (PCs; PC1, x-axis; PC2, y-axis) representing the largest variance in the dataset. Each component is a linear combination of 94 immune genes (figure 1A). Compared with samples from CLE-U and HVs, CLE-A were shifted forward on the x-axis of PC1, accounting for 60% of the total variance in the dataset. Within disease groups, CLE-A and CLE-U were separated from one another (figure 1A). HVs were shifted slightly backward along PC1.

Expression analysis (K-means) revealed four gene clusters

After determining that tape-derived RNA gene expression from a 94-candidate gene panel could distinguish disease groups, we sought to compile gene clusters with the greatest potential to differentiate between CLE and HV groups. We examined gene expression across all groups using the consensus of 1000 K-means clustering results from bootstrapping. Genes amplified from skin tape-collected RNA were segregated into four clusters, as shown in figure 1B.

We then examined the differential between the mean expression of each cluster in CLE-A versus HV and in CLE-A versus CLE-U (online supplemental table S8). Two of four clusters resulted in differential expression for both comparisons (figure 1B): cluster 3, IFN dominant included 14/18 genes in the cluster that were IFN responsive; and cluster 1, or CLE associated, was composed of a mixture of genes implicated in CLE pathogenesis. The IFN-dominant cluster (cluster 3) differentiated CLE-A from HV (23-fold change; p<0.001) and CLE-U (eightfold

Table 1 Participant characteristics

	HV (n=10)	DLE (n=9)	SCLE (n=1)
Age (years), mean (SD)	55.7 (5.4)	56.0 (12.0)	58.0 (NC)
Female, n (%)	5 (50)	7 (78)	1 (100)
Body mass index (kg/m^2), mean (SD)	28.1 (6.2)	28.1 (4.4)	35.1 (NC)
Race, n (%)			
American Indian or Alaskan Native	1 (10)	0	0
Asian	0	0	0
Black or African-American	0	3 (33)	0
White	9 (90)	6 (67)	1 (100)
Concomitant SLE per ACR criteria, n	N/A	3	0
Concomitant medication, n (%)	0	7 (78)	1 (100)
Hydroxychloroquine	0	5 (56)	1 (100)
Prednisone	0	2 (22)	0
Corticosteroid NOS	0	3 (33)	0
Clobetasol propionate	0	2 (22)	0
Fluocinonide	0	1 (11)	0
Hydrocortisone	0	0	0
Mycophenolate mofetil	0	1 (11)	1 (100)
Tacrolimus	0	0	1 (100)
Disease activity			
PGA (mm), mean (range)	N/A	13.3 (10–30)	20
CLASI-A, mean (range)	N/A	11.8 (4–19)	11

ACR, American College of Rheumatology; CLASI-A, Cutaneous Lupus Area and Severity Index-activity; DLE, discoid lupus erythematosus; HV, healthy volunteer; N/A, not applicable; NC, not calculable; NOS, not otherwise specified; PGA, Physician Global Assessment; SCLE, subacute cutaneous lupus erythematosus.

change; p=0.002), respectively (figure 2A). The CLE-associated cluster (cluster 1) differentiated CLE-A from HV (fourfold change; p=0.005) and CLE-U (fourfold change; p=0.012), respectively (figure 2B). A third gene cluster (cluster 2) composed of a mixture of IFN-associated and CLE-associated genes (CLE2-associated cluster) also distinguished CLE-A from HV skin (three-fold change; p=0.001) but for this cluster, the difference between CLE-A and CLE-U did not reach the level of significance (online supplemental figure S2A and S2B).

Ingenuity pathway analysis

To explore the relationship between gene clusters found by differential expression between disease groups and their commonly cited pathways in the literature, we used Ingenuity Pathway Analysis (Invitrogen, Carlsbad, California, USA). Analysis of cluster 1 (CLE-associated genes) revealed significant associations with pathways involved in communication between innate and adaptive immune cells, *TREM1* signalling and granulocyte adhesion and diapedesis (online supplemental table S9). Analysis of cluster 3 (IFN dominant) revealed associations between genes in the IFN-signalling pathway and the role of hypercytokinaemia/hyperchemokinaemia in the pathogenesis of influenza and pathways associated with pattern recognition receptors that detect bacteria and viruses (online supplemental table S9).

Heat map of gene-level expression

To examine the contribution of individual genes to clusters 1 and 3, we developed a heat map of gene-level expression relative to the mean of the HV samples. The greatest individual gene log2 fold change above the mean of the HV was visualised in the CLE-A disease group versus the HV group in the IFN gene cluster (range, 3.1–5.9; figure 3). Unsurprisingly, genes with the strongest differential between CLE-A and the mean of the HV were *IFI6*, *IFI44*, *MX1* and *USP18* (range, 5.5–5.9), all of which are IFN response genes. A strong differential was also seen between CLE-A and CLE-U in the IFN cluster. There was a less robust differential between CLE-A and the mean of the HV in the CLE-associated cluster (range, 1.4–3.8), for example, *ISG15*, *GZMB* and *ITGAX* with log2 fold changes ranging from 3.3 to 3.8, and a weak differential between CLE-A and CLE-U in the CLE-associated cluster.

Differential expression of interferon genes in skin versus blood

Given the robust differential IFN gene signature in CLE skin, we explored whether expression of IFN genes in

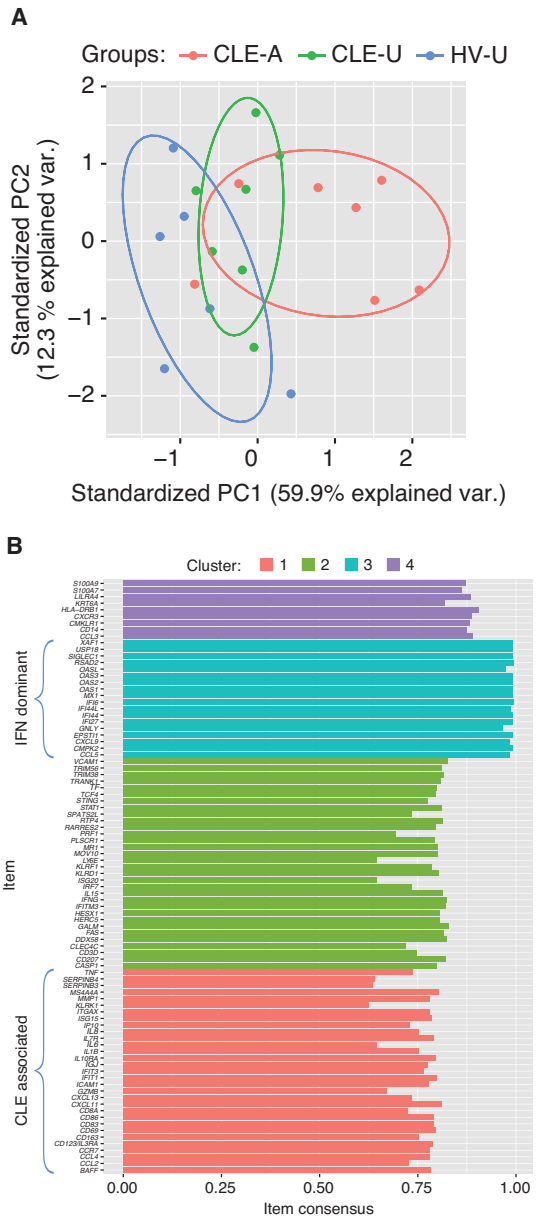

Figure 1 Principal component (PC) analysis separates disease groups, and unbiased K-means clustering segregates genes by differential gene expression. (A) PC analysis. Using RNA collected with tape and relative expression of 94 immune genes, participants with CLE are differentiated from HVs. Compared with unaffected skin from participants with CLE and HVs, CLE-affected skin is shifted forward on the x-axis of PC1. (B) K-means clustering of expression for 94 candidate genes. Expression of genes amplified from skin RNA collected with tape was segregated into four clusters. Two of four clusters resulted in differential expression between both CLE-affected skin and HV, and between CLE-affected skin and CLE-unaffected skin: cluster 3, named interferon (IFN) dominant, and cluster 1, named CLE associated. Item consensus (x-axis) represents the percentage of instances that expression of a gene falls within the represented cluster after bootstrapping 1000 times. CLE-A, cutaneous lupus erythematosus-affected skin; CLE-U, cutaneous lupus erythematosus-unaffected skin; HV-U, healthy volunteer-unaffected skin; var, variance.

blood would discriminate between participants with CLE and HVs. For this analysis, we used an abbreviated 22-gene IFN signature[20] to measure the gene expression in paired blood-derived and skin tape-derived RNA samples from five participants with CLE (online supplemental table S10).

Mean change in IFN gene expression between CLE and HV was sevenfold (p=0.016) in whole blood RNA and ninefold (p=0.002) in skin tape-derived RNA (online supplemental figure S3). Mean change in gene expression between CLE-A and CLE-U in skin tape-derived RNA was fourfold (p=0.010; online supplemental figure S3). These data indicate that in patients presenting with active CLE skin lesions, skin tape-derived RNA may be as sensitive—perhaps even more sensitive—than blood RNA for the assessment of IFN gene signature expression.

Correlation of myxovirus resistance protein A, CD45 and CD303 protein quantification

As the traditional method of assessing biomarkers in CLE lesions is punch biopsy followed by IHC, we selected three tissue-based protein biomarkers of CLE activity for comparison with IFN-associated and CLE-associated gene clusters from skin tape-derived RNA. We performed IHC on biopsies taken at the same site as the CLE-A skin tape-derived RNA samples for the following: MXA (annotated as MX1 in RNA clusters), an IFN modulated protein; CD45, for inflammatory infiltrates and CD303 (BDCA-2), a receptor uniquely expressed on pDCs. On images derived from IHC slides, we annotated epidermis and dermis, and compared immunoreactive tissue area for each biomarker by disease group (figure 4, online supplemental figure S4A).

As expected, the MXA immunoreactive area was large and diffusely distributed throughout the epidermis in participants with CLE, with less robust multifocal immunoreactivity in the dermis. MXA expression ranged from very low to absent in HVs. A Spearman's correlation between per cent area of MXA immunoreactivity and IFN mRNA gene cluster expression was highly significant (dermis, rho=0.86, p<0.001; figure 4A). As most of the IFN gene cluster comprised IFN response genes, including MXA, and MXA is expressed in the epidermis, this result was expected and indicated that tape-derived RNA offers a potential surrogate for MXA protein quantification in punch biopsies.

The CD45 immunoreactive area was most robust in the dermis, with a multifocal distribution, found in participants with CLE and at very low levels in HV skin. Per cent CD45 immunoreactive area correlated with IFN mRNA gene cluster expression (dermis, rho=0.74, p=0.002; online supplemental figure S4B). Across disease groups there was enough of a dynamic range in CD45 immunoreactivity and IFN gene expression to provide a positive correlation between these biomarkers.

CD303 immunoreactive area was greatest in participants with CLE, with a multifocal distribution in dermis tracking along with inflammatory infiltrates. CD303 was

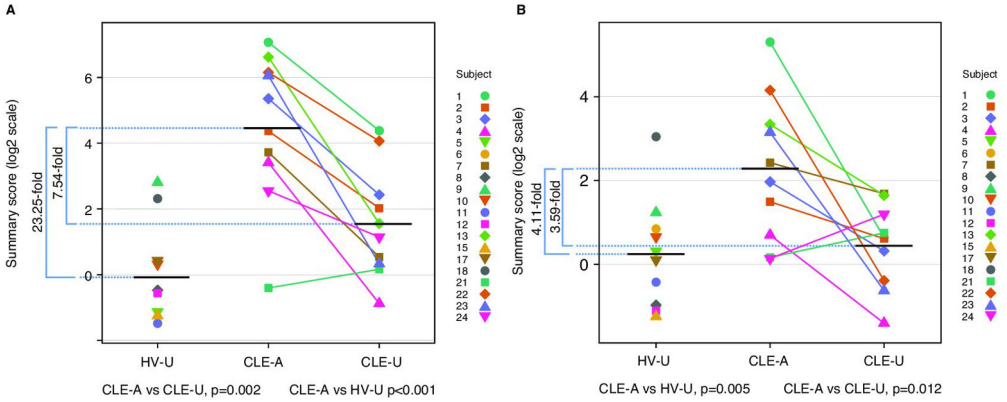

Figure 2 Summary scores for interferon-associated and CLE-associated gene clusters differentiate HVs from CLE-A and CLE-A versus CLE-U groups. Gene expression in CLE-affected skin, CLE-unaffected skin and HVs for (A) the interferon-dominant gene cluster (cluster 3) and (B) the CLE-associated gene cluster (cluster 1). Each coloured symbol represents a single participant. CLE-A, cutaneous lupus erythematosus-affected skin; CLE-U, cutaneous lupus erythematosus-unaffected skin; HV-U, healthy volunteer-unaffected skin.

very low in HVs. Per cent area of CD303 immunoreactivity strongly correlated with IFN mRNA gene cluster expression (dermis, rho=0.84, p<0.001; figure 4B).

Using the CLE-associated gene cluster, correlations with MXA and CD45 immunoreactive areas were also statistically significant (online supplemental figure S5).

DISCUSSION

This pilot study was designed to assess if a tape device (https://dermtech.com) used in the clinic for melanoma diagnosis[36 37] could identify gene signatures relevant to CLE pathogenesis and be used as a tool to monitor CLE biomarkers and potentially replace punch biopsy in the clinical research setting. Using skin tape mRNA collection, two gene clusters were identified with differential expression in CLE-A versus CLE-U and HV skin. Gene expression in these two clusters, IFN-associated and CLE-associated, correlated with MXA, CD45 and CD303, and with MXA and CD45, respectively, protein in punch biopsies by immunoreactive tissue area.

In this study, candidate genes were selected based on their association with CLE pathogenesis, and were enriched with IFN pathway genes likely to distinguish between CLE-A and CLE-U skin. As expected, IFN response genes were plentiful in clusters 1 and 3, the gene clusters with the strongest differential in mean expression between CLE-A and HV, and between CLE-A and CLE-U lesions.

Our finding that IFN pathway genes recovered by tape harvesting distinguish between CLE-A and CLE-U or HV skin is supported in the CLE transcriptomics literature.[44–50] Many of the IFN response genes with highest ranking fold changes in previous studies are also differentially regulated in this tape-derived RNA study. These include *IFI27, IFI44L, IFI44, OAS1* (blood from participants with CLE),[44] *CCL5, CXCL9, Mx1, OAS2* and *AIM2* (affected skin biopsies from participants with CLE)[45 46 50] and *Mx1, IFI6, OAS2, XAF1, CXCL10* and *IFI27* (follicular epithelium from participants with CLE).[47]

Previous evidence also underpins an important role for cytotoxic NK cell-mediated and T cell-mediated apoptosis in CLE pathogenesis.[19 45 51] In support of this hypothesis, in CLE transcript profiling studies comparing CLE lesions with unaffected skin or with HV skin using full-thickness skin biopsy[45] or follicular epithelium from plucked hairs,[47] upregulated IFN response genes included the apoptosis-related *XAF1, OAS1* and *OAS2,* consistent with our findings. Also convergent with our findings, in previous CLE transcriptome studies, genes expressed in cytotoxic NK and T cells were upregulated, including *FAS, GZMB, PRF1* and *GNLY*.[45] The presence of vacuolar degeneration along the basal epidermis due to degenerating and apoptotic keratinocytes is a hallmark of CLE histological diagnosis, highlighting a prominent role for apoptosis and cell-mediated keratinocyte killing in the interface dermatitis characteristic of CLE.

This pilot study was designed to evaluate a tape device as a potential tool in clinical trials to monitor CLE biomarkers that are relevant to CLE pathogenesis. Although limited by a small sample size, results indicated that material of sufficient quality and quantity was obtained to provide relevant information on IFN-associated or CLE-associated gene signature detection. However, additional study is warranted to confirm sensitivity and/or specificity of the skin tape device for use in large efficacy clinical trials in CLE. Previous experience of this skin tape RNA device (Dermtech, La Jolla, California, USA) in the diagnosis of melanoma demonstrated 91% sensitivity and 69% specificity. This device is currently used in clinical practice to confirm the diagnosis of melanoma.[36 37]

Although differential RNA expression from cytotoxic NK-cell and T-cell genes was observed in this tape RNA study, we cannot rule out the possibility that blood contamination of skin tape-derived RNA samples may have introduced RNA from circulating cells.

We noted that the fold change in IFN pathway genes is more pronounced in skin tape samples than in whole blood. This finding is supported by earlier work, in which

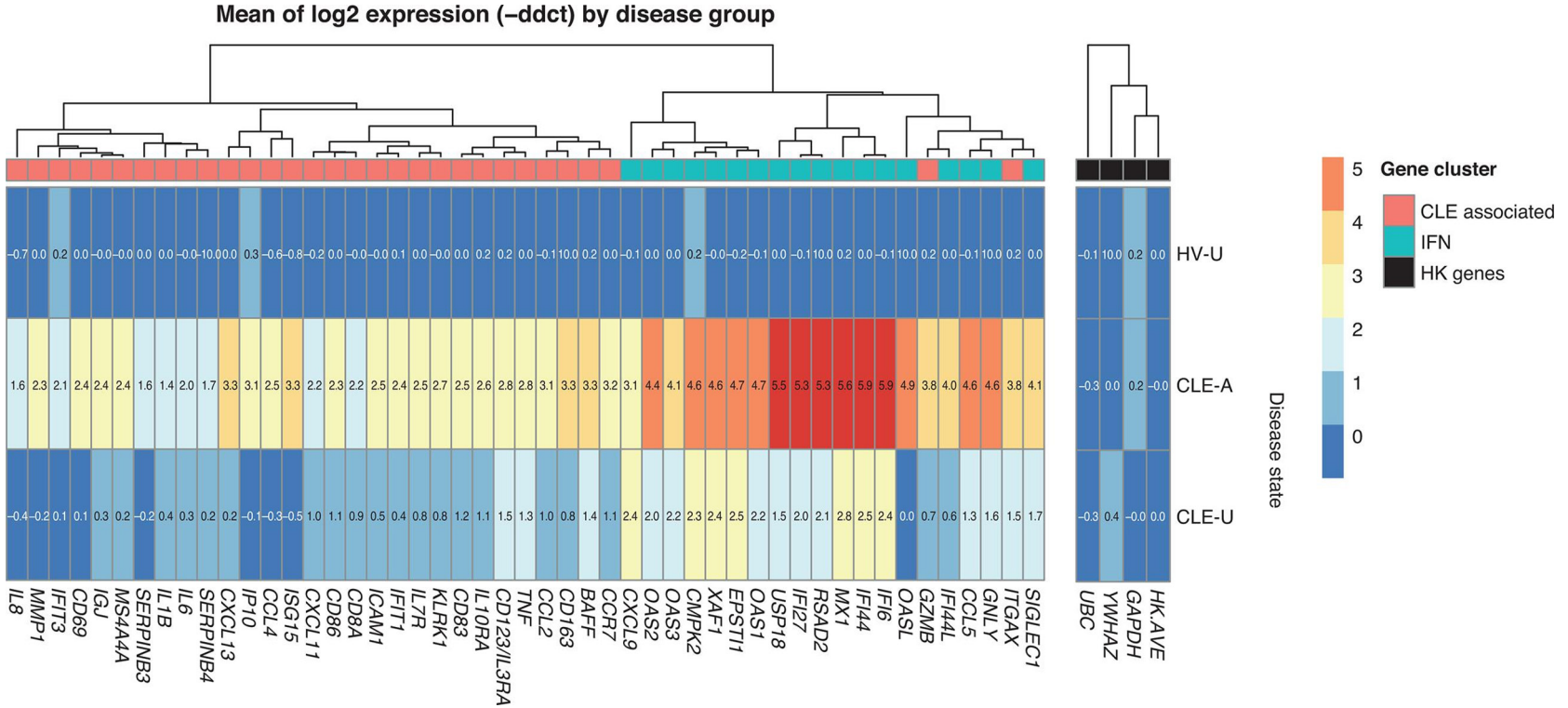

Figure 3 Heat map of interferon (IFN)-associated and CLE-associated gene expression by disease group. Log2 fold change from the mean of HV for each gene in the IFN-associated (blue boxes in top row) and CLE-associated (red boxes in top row) clusters. Log2 fold change for three housekeeping (HK) genes (*GAPDH, UBC, YWHAZ*), and the average log2 fold change for these three HK genes (HK.AVE), are shown (black boxes in top row). Log2 fold changes are given by colour (red, increased; dark blue, decreased) and by value in each cell. Relatedness of gene expression log2 fold changes is depicted with a dendrogram across the top of the figure. Disease groups are listed along the y-axis. Genes are listed along the x-axis. CLE-A, cutaneous lupus erythematosus-affected skin; CLE-U, cutaneous lupus erythematosus-unaffected skin; HV-U, healthy volunteer-unaffected skin.

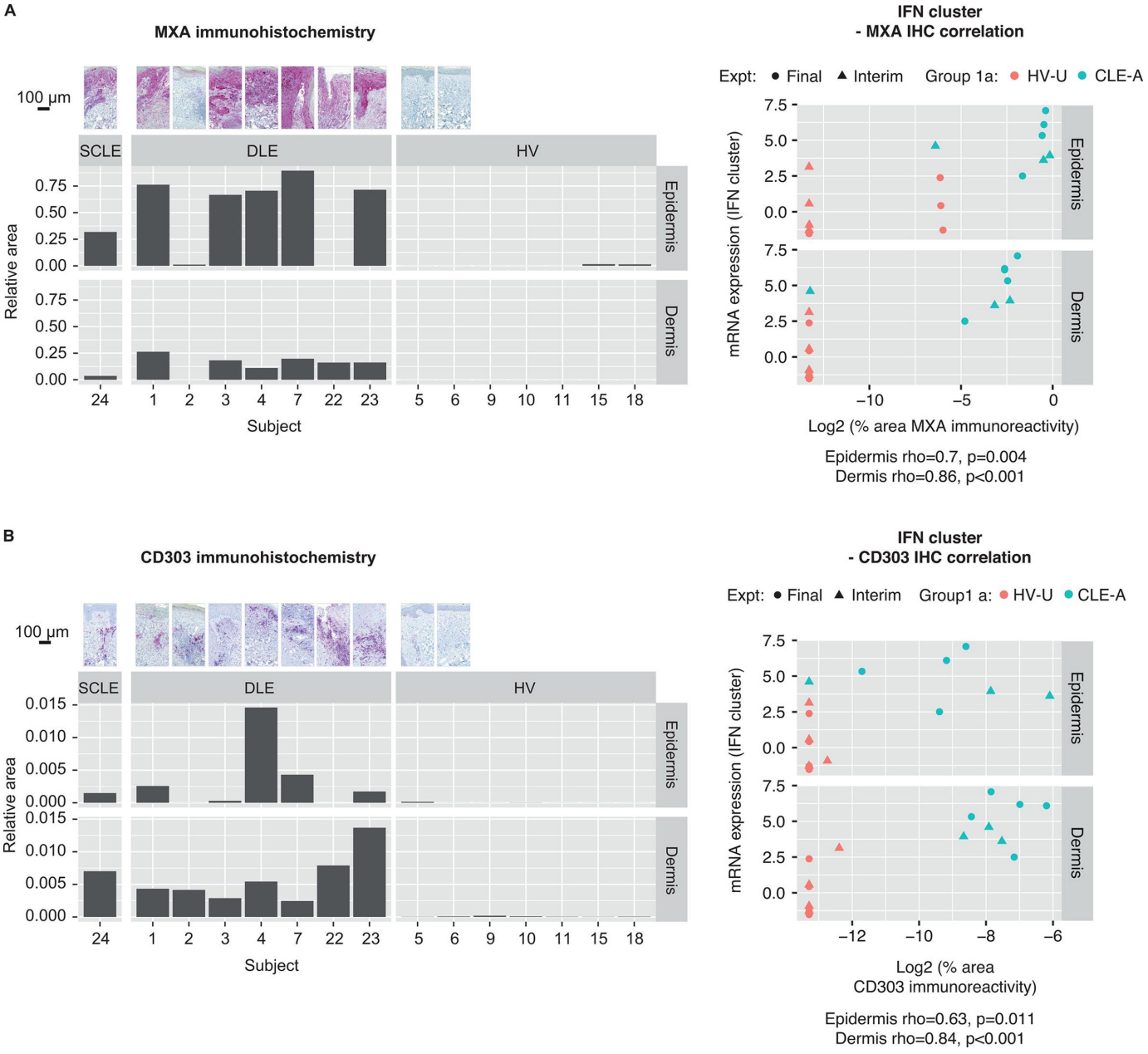

Figure 4 An interferon (IFN)-dominant gene signature is correlated with a hallmark IFN-response protein (A) myxovirus resistance protein A (MXA) and (B) CD303^{+} plasmacytoid dendritic cells demonstrated by immunoreactivity in punch biopsies. Representative photomicrographs of immunohistochemistry (IHC) for MXA and CD303, bar graphs with their quantification and Spearman's correlations between each IHC biomarker and the IFN RNA summary score. CLE-A, cutaneous lupus erythematosus-affected skin; DLE, discoid lupus erythematosus; Expt, experiment; HV, healthy volunteer; HV-U, healthy volunteer-unaffected skin; mRNA, messenger RNA; SCLE, subacute cutaneous lupus erythematosus.

after unsupervised clustering, skin CLE samples separated out from blood CLE samples along the first three PCs.[48] Additionally, specific Kyoto Encyclopaedia of Genes and Genomes pathways were enriched in the skin compared with blood.[48]

There are two, non-mutually exclusive mechanisms to explain the finding that mean fold change of IFN genes was higher in skin relative to whole blood involving either pDCs and associated inflammatory infiltrates and/or keratinocytes. In subjects with SLE, pDC numbers are decreased in blood.[11] By contrast, pDC numbers are increased in target organs including kidney[52 53] and skin.[54 55] pDCs isolated from CLE skin biopsies express multiple IFN-α subtypes, IFN-β and IFN-ε.[56] As potent producers of IFN, localised, tissue-based enrichment of pDCs as part of an inflammatory infiltrate also expressing elevated levels of IFN-induced genes[19 57] may contribute to enhancement of IFN-stimulated gene expression in the target organ. In addition, cross-talk among the cells involved in CLE dermatitis, including NK, B and T, myeloid and pDCs may promote increased expression of IFN by pDCs and keratinocytes.[19 58–60]

Keratinocytes produce type I IFNs including IFN-κ,[39] important in the potentiation of epidermal IFN production in CLE skin lesions.[38] In addition to IFN-I, keratinocytes produce type III IFNs.[13] In an IHC study, epidermal immunoreactivity for IFN-λ and the IFN-λ receptor was increased in SCLE and DLE lesions versus lesions from other inflammatory skin diseases and healthy participants.[13] As an additional source of IFN-λ, it has been shown in a study with *ex vivo* peripheral blood mononuclear cell cultures that TLR9 ligand (CpG-A)-induced IFN-λ secretion is decreased on treatment with BIIB059,[20] which binds to BDCA2,[61] a receptor unique to pDCs. In keratinocytes, both IFN-κ and IFN-λ signal via their receptors through the Jak/STAT pathway in common with IFN-α, resulting in overlapping IFN gene response signatures, so both IFN-I and IFN-III could contribute to the differential gene expression in CLE-affected skin versus blood reported here.[62]

Related to the above mechanisms leading to localised differential expression of IFN genes, we observed increased gene expression of both IFN-associated and CLE-associated gene clusters in affected skin compared with unaffected skin. In unaffected skin, IFN-associated and CLE-associated gene expression was not at the same level as HV, rather the expression level was intermediate between affected skin and HV skin, similar to what has been reported in AD[33 63] and psoriasis.[34] The finding of an intermediate level of IFN-associated and CLE-associated gene expression in unaffected CLE skin may indicate that there is a low level of inflammation not discernible by gross morphological change.

To our knowledge, no publications describing a comparison between tape-derived and biopsy-derived gene expression are available in CLE. Such studies are published in AD and psoriasis. The two modalities yielded distinct yet overlapping results. Kim *et al* showed that expression of terminal epidermal differentiation markers in tape-derived HV and AD samples correlated with expression of the same markers in adjacent biopsy.[32] Dyjack *et al* found that in non-lesional AD skin, there was more overlap between skin tape and biopsied epidermis than between either skin tape and biopsied dermis or biopsied epidermis and biopsied dermis.[33] Highlighting the relevance of tape sampling for inflammatory skin disease, in an AD type 2 high endotype the most highly differentially expressed genes detected by skin tape were related to activation of T_H2 and DC pathways.[33] He *et al*[34] found that tape-derived transcriptomes analyses from patients with AD and psoriasis were correlated with a previously published transcriptome biopsy dataset. Interestingly, tape transcriptomes from AD non-lesional skin showed greater fold changes than biopsy specimens for both AD and psoriasis, with tape RNA showing significant upregulation of T_H2 products (CCL17/TARC and TNFRSF4/OX40) not found in biopsy specimens.[34] Taken together, these data indicate that tape-derived RNA yields distinct and overlapping results relative to biopsy-derived RNA, and certain biomarkers can be assessed by tape RNA in better resolution than biopsy-derived RNA.

In this pilot study, we demonstrate the ability of IFN-associated and CLE-associated gene clusters to distinguish between CLE-A and CLE-U, and HV skin. These data indicate that tape-derived RNA is a potential tool to monitor biomarkers in longitudinal CLE studies, although a study with a larger sample size is warranted to confirm the validity of this approach in CLE.

Author affiliations
[1]Department of Dermatology and Department of Medicine, Division of Rheumatology, Brigham and Women's Hospital, Boston, Massachusetts, USA
[2]Harvard Medical School, Boston, Massachusetts, USA
[3]Biogen Inc, Cambridge, Massachusetts, USA
[4]Dermatology, Boston University, Boston, Massachusetts, USA
[5]Biogen Switzerland AG, Baar, Switzerland

Acknowledgements The authors would like to thank the following for their valuable contributions: Zuxu Yao and Talisha Allen from DermTech, Inc., Robert Dunstan, Huo Li, David Martin, Norman Allaire, Marian Themeles, Anne Ranger, Amy Kao, Kejie Li and Margaret Choy Merola. The authors wrote the first draft of the manuscript and Linda Wagner of Excel Scientific Solutions provided editorial support. Miranda Dixon from Excel Scientific Solutions copyedited and styled the manuscript.

Contributors Conceptualisation: CB, TLR, NF, JFM, DR. Data curation: CGW, TLR, SH. Formal analysis: CGW, WW, TLR. Funding acquisition: NF. Investigation: TLR, CL, JFM, AT, SH, XZ. Methodology: CGW, WW, TLR, GM, XZ. Project administration: CM, CB, TLR, GM. Software: CGW, SH. Supervision: CB, TLR, NF. Validation: TLR. Visualisation: CGW, WW, CB, TLR. Writing—original draft preparation: CB, WW, TLR, JFM. Writing—review and editing: CGW, WW, CB, TLR, CL, NF, JFM, AT, GM, DR, XZ, SH, CR, CM.

Funding Biogen sponsored this study. Biogen provided funding for medical writing support in the development of this manuscript. Biogen reviewed and provided feedback on the article to the authors.

Competing interests JFM is a consultant and/or investigator for AbbVie, Aclaris, Almirall, Avotres, Biogen, Celgene, Dermavant, EMD Serono, Incyte, Janssen, Leo, Lilly, Merck, Novartis, Pfizer, Sanofi Regeneron, Sun and UCB. WW, SH, AT, CM, GM, CB, NF and TLR are employees and shareholders of Biogen. CGW, XZ, CR and DR are former employees of Biogen. XZ, CR and DR are now employees of Vertex, Genomics Institute of the Novartis Research Foundation and Rheos Medicines, respectively. CL has been an investigator for Biogen. NF serves on the board of OMass Therapeutics.

Patient consent for publication Not required.

Ethics approval This study was conducted in accordance with the Declaration of Helsinki and other ethical principles described in Title 45, United States Code of Federal Regulations Part 46, Subparts A and B, and approved by the institutional review boards at Brigham and Women's Hospital (approval ID # 2013P002615/MGH) and Boston University School of Medicine (approval ID # H-34177). Written informed consent was obtained from all participants. The study started on 6 May 2014 and completed on 26 May 2016.

Provenance and peer review Not commissioned; externally peer reviewed.

Data availability statement Requests for data supporting this manuscript should be submitted to the Biogen Clinical Data Request Portal (http://clinicalresearch.biogen.com).

ORCID iD

Taylor L Reynolds http://orcid.org/0000-0002-6941-0900

REFERENCES

1 Jarrett P, Werth VP. A review of cutaneous lupus erythematosus: improving outcomes with a multidisciplinary approach. *J Multidiscip Healthc* 2019;12:419–28.
2 Okon LG, Werth VP. Cutaneous lupus erythematosus: diagnosis and treatment. *Best Pract Res Clin Rheumatol* 2013;27:391–404.
3 Stannard JN, Kahlenberg JM. Cutaneous lupus erythematosus: updates on pathogenesis and associations with systemic lupus. *Curr Opin Rheumatol* 2016;28:453–9.
4 Achtman JC, Werth VP. Pathophysiology of cutaneous lupus erythematosus. *Arthritis Res Ther* 2015;17:182.
5 Lichtman EI, Helfgott SM, Kriegel MA. Emerging therapies for systemic lupus erythematosus--focus on targeting interferon-alpha. *Clin Immunol* 2012;143:210–21.
6 Baechler EC, Batliwalla FM, Karypis G, *et al*. Interferon-inducible gene expression signature in peripheral blood cells of patients with severe lupus. *Proc Natl Acad Sci U S A* 2003;100:2610–5.
7 Bennett L, Palucka AK, Arce E, *et al*. Interferon and granulopoiesis signatures in systemic lupus erythematosus blood. *J Exp Med* 2003;197:711–23.
8 Chiche L, Jourde-Chiche N, Whalen E, *et al*. Modular transcriptional repertoire analyses of adults with systemic lupus erythematosus reveal distinct type I and type II interferon signatures. *Arthritis Rheumatol* 2014;66:1583–95.
9 Crow MK, Kirou KA, Wohlgemuth J. Microarray analysis of interferon-regulated genes in SLE. *Autoimmunity* 2003;36:481–90.
10 Langefeld CD, Ainsworth HC, Cunninghame Graham DS, *et al*. Transancestral mapping and genetic load in systemic lupus erythematosus. *Nat Commun* 2017;8:16021.
11 Nehar-Belaid D, Hong S, Marches R, *et al*. Mapping systemic lupus erythematosus heterogeneity at the single-cell level. *Nat Immunol* 2020;21:1094–106.
12 Rice GI, Melki I, Frémond M-L, *et al*. Assessment of type I interferon signaling in pediatric inflammatory disease. *J Clin Immunol* 2017;37:123–32.
13 Zahn S, Rehkämper C, Kümmerer BM, *et al*. Evidence for a pathophysiological role of keratinocyte-derived type III interferon (IFNλ) in cutaneous lupus erythematosus. *J Invest Dermatol* 2011;131:133–40.
14 Banchereau R, Hong S, Cantarel B, *et al*. Personalized immunomonitoring uncovers molecular networks that stratify lupus patients. *Cell* 2016;165:551–65.
15 Chaussabel D, Quinn C, Shen J, *et al*. A modular analysis framework for blood genomics studies: application to systemic lupus erythematosus. *Immunity* 2008;29:150–64.
16 Kirou KA, Lee C, George S, *et al*. Activation of the interferon-alpha pathway identifies a subgroup of systemic lupus erythematosus patients with distinct serologic features and active disease. *Arthritis Rheum* 2005;52:1491–503.
17 Braunstein I, Klein R, Okawa J, *et al*. The interferon-regulated gene signature is elevated in subacute cutaneous lupus erythematosus and discoid lupus erythematosus and correlates with the cutaneous lupus area and severity index score. *Br J Dermatol* 2012;166:971–5.
18 Yao Y, Higgs BW, Richman L, *et al*. Use of type I interferon-inducible mRNAs as pharmacodynamic markers and potential diagnostic markers in trials with sifalimumab, an anti-IFNα antibody, in systemic lupus erythematosus. *Arthritis Res Ther* 2010;12 Suppl 1:S6.
19 Wenzel J, Zahn S, Mikus S, *et al*. The expression pattern of interferon-inducible proteins reflects the characteristic histological distribution of infiltrating immune cells in different cutaneous lupus erythematosus subsets. *Br J Dermatol* 2007;157:752–7.
20 Furie R, Werth VP, Merola JF, *et al*. Monoclonal antibody targeting BDCA2 ameliorates skin lesions in systemic lupus erythematosus. *J Clin Invest* 2019;129:1359–71.
21 Furie R, Khamashta M, Merrill JT, *et al*. Anifrolumab, an anti-interferon-α receptor monoclonal antibody, in moderate-to-severe systemic lupus erythematosus. *Arthritis Rheumatol* 2017;69:376–86.
22 Khamashta M, Merrill JT, Werth VP, *et al*. Sifalimumab, an anti-interferon-α monoclonal antibody, in moderate to severe systemic lupus erythematosus: a randomised, double-blind, placebo-controlled study. *Ann Rheum Dis* 2016;75:1909–16.
23 Morand EF, Furie R, Tanaka Y, *et al*. Trial of anifrolumab in active systemic lupus erythematosus. *N Engl J Med* 2020;382:211–21.
24 Werth V, Furie R, Romero-Diaz J. OP0193 BIIB059, a humanized monoclonal antibody targeting BDCA2 on plasmacytoid dendritic cells (pDC), shows dose-related efficacy in the phase 2 LILAC study in patients (pts) with active cutaneous lupus erythematosus (CLE). *Ann Rheum Dis* 2020;79:120–1.
25 Werth V, Furie R, Romero-Díaz J. BIIB059, a humanized monoclonal antibody targeting blood dendritic cell antigen 2 on plasmacytoid dendritic cells, shows dose-related efficacy in a phase 2 study in participants with active cutaneous lupus erythematosus [abst # 0986]. *Arthritis Rheumatol* 2020;72.
26 Sticherling M, Bonsmann G, Kuhn A. Diagnostic approach and treatment of cutaneous lupus erythematosus. *J Dtsch Dermatol Ges* 2008;6:48–59.
27 Kadouch DJ, Leeflang MM, Elshot YS, *et al*. Diagnostic accuracy of confocal microscopy imaging vs. punch biopsy for diagnosing and subtyping basal cell carcinoma. *J Eur Acad Dermatol Venereol* 2017;31:1641–8.
28 Morhenn VB, Chang EY, Rheins LA. A noninvasive method for quantifying and distinguishing inflammatory skin reactions. *J Am Acad Dermatol* 1999;41:687–92.
29 Benson NR, Papenfuss J, Wong R, *et al*. An analysis of select pathogenic messages in lesional and non-lesional psoriatic skin using non-invasive tape harvesting. *J Invest Dermatol* 2006;126:2234–41.
30 Wong R, Tran V, Morhenn V, *et al*. Use of RT-PCR and DNA microarrays to characterize RNA recovered by non-invasive tape harvesting of normal and inflamed skin. *J Invest Dermatol* 2004;123:159–67.
31 Yao Z, Moy R, Allen T, *et al*. An adhesive patch-based skin biopsy device for molecular diagnostics and skin microbiome studies. *J Drugs Dermatol* 2017;16:979–86.
32 Kim BE, Goleva E, Kim PS, *et al*. Side-by-side comparison of skin biopsies and skin tape stripping highlights abnormal stratum corneum in atopic dermatitis. *J Invest Dermatol* 2019;139:2387–9.
33 Dyjack N, Goleva E, Rios C, *et al*. Minimally invasive skin tape strip RNA sequencing identifies novel characteristics of the type 2-high atopic dermatitis disease endotype. *J Allergy Clin Immunol* 2018;141:1298–309.
34 He H, Bissonnette R, Wu J, *et al*. Tape strips detect distinct immune and barrier profiles in atopic dermatitis and psoriasis. *J Allergy Clin Immunol* 2021;147:199–212.
35 Wachsman W, Morhenn V, Palmer T, *et al*. Noninvasive genomic detection of melanoma. *Br J Dermatol* 2011;164:797–806.
36 Gerami P, Yao Z, Polsky D, *et al*. Development and validation of a noninvasive 2-gene molecular assay for cutaneous melanoma. *J Am Acad Dermatol* 2017;76:114–20.
37 Ferris LK, Jansen B, Ho J, *et al*. Utility of a noninvasive 2-gene molecular assay for cutaneous melanoma and effect on the decision to biopsy. *JAMA Dermatol* 2017;153:675–80.
38 Sarkar MK, Hile GA, Tsoi LC, *et al*. Photosensitivity and type I IFN responses in cutaneous lupus are driven by epidermal-derived interferon kappa. *Ann Rheum Dis* 2018;77:1653–64.
39 Stannard JN, Reed TJ, Myers E, *et al*. Lupus Skin Is Primed for IL-6 Inflammatory Responses through a Keratinocyte-Mediated Autocrine Type I Interferon Loop. *J Invest Dermatol* 2017;137:115–22.
40 Tsoi LC, Hile GA, Berthier CC, *et al*. Hypersensitive IFN responses in lupus keratinocytes reveal key mechanistic determinants in cutaneous lupus. *J Immunol* 2019;202:2121–30.
41 Klein R, Moghadam-Kia S, LoMonico J, *et al*. Development of the CLASI as a tool to measure disease severity and responsiveness to therapy in cutaneous lupus erythematosus. *Arch Dermatol* 2011;147:203–8.
42 Hochberg MC. Updating the American College of rheumatology revised criteria for the classification of systemic lupus erythematosus. *Arthritis Rheum* 1997;40:1725.
43 Tan EM, Cohen AS, Fries JF, *et al*. The 1982 revised criteria for the classification of systemic lupus erythematosus. *Arthritis Rheum* 1982;25:1271–7.
44 Dey-Rao R, Sinha AA. Genome-wide transcriptional profiling of chronic cutaneous lupus erythematosus (CCLE) peripheral blood identifies systemic alterations relevant to the skin manifestation. *Genomics* 2015;105:90–100.
45 Dey-Rao R, Smith JR, Chow S, *et al*. Differential gene expression analysis in CCLE lesions provides new insights regarding the genetics basis of skin vs. systemic disease. *Genomics* 2014;104:144–55.

46 Jabbari A, Suárez-Fariñas M, Fuentes-Duculan J, *et al*. Dominant Th1 and minimal Th17 skewing in discoid lupus revealed by transcriptomic comparison with psoriasis. *J Invest Dermatol* 2014;134:87–95.
47 Shalbaf M, Alase AA, Berekmeri A, *et al*. Plucked hair follicles from patients with chronic discoid lupus erythematosus show a disease-specific molecular signature. *Lupus Sci Med* 2019;6:e000328.
48 Sinha AA, Dey-Rao R. Genomic investigation of lupus in the skin. *J Investig Dermatol Symp Proc* 2017;18:S75–80.
49 Berthier CC, Tsoi LC, Reed TJ, *et al*. Molecular profiling of cutaneous lupus lesions identifies subgroups distinct from clinical phenotypes. *J Clin Med* 2019;8:1244.
50 Fetter T, Smith P, Guel T, *et al*. Selective janus kinase 1 inhibition is a promising therapeutic approach for lupus erythematosus skin lesions. *Front Immunol* 2020;11:344.
51 Toberer F, Sykora J, Göttel D, *et al*. Apoptotic signal molecules in skin biopsies of cutaneous lupus erythematosus: analysis using tissue microarray. *Exp Dermatol* 2013;22:656–9.
52 Tucci M, Quatraro C, Lombardi L, *et al*. Glomerular accumulation of plasmacytoid dendritic cells in active lupus nephritis: role of interleukin-18. *Arthritis Rheum* 2008;58:251–62.
53 Arazi A, Rao DA, Berthier CC, *et al*. The immune cell landscape in kidneys of patients with lupus nephritis. *Nat Immunol* 2019;20:902–14.
54 Blomberg S, Eloranta ML, Cederblad B, *et al*. Presence of cutaneous interferon-alpha producing cells in patients with systemic lupus erythematosus. *Lupus* 2001;10:484–90.
55 Farkas L, Beiske K, Lund-Johansen F, *et al*. Plasmacytoid dendritic cells (natural interferon-alpha/beta-producing cells) accumulate in cutaneous lupus erythematosus lesions. *Am J Pathol* 2001;159:237–43.
56 Gardet A, Carlile T, Chou W. Comprehensive characterization of the immune infiltrate of skin biopsies from cutaneous lupus erythematosus patients using single cell RNAseq [abst # 1931]. *Arthritis Rheumatol* 2019;71.
57 Blanco P, Palucka AK, Gill M, *et al*. Induction of dendritic cell differentiation by IFN-alpha in systemic lupus erythematosus. *Science* 2001;294:1540–3.
58 Hagberg N, Berggren O, Leonard D, *et al*. IFN-α production by plasmacytoid dendritic cells stimulated with RNA-containing immune complexes is promoted by NK cells via MIP-1β and LFA-1. *J Immunol* 2011;186:5085–94.
59 Berggren O, Hagberg N, Weber G, *et al*. B lymphocytes enhance interferon-α production by plasmacytoid dendritic cells. *Arthritis Rheum* 2012;64:3409–19.
60 Leonard D, Eloranta M-L, Hagberg N, *et al*. Activated T cells enhance interferon-α production by plasmacytoid dendritic cells stimulated with RNA-containing immune complexes. *Ann Rheum Dis* 2016;75:1728–34.
61 Pellerin A, Otero K, Czerkowicz JM, *et al*. Anti-BDCA2 monoclonal antibody inhibits plasmacytoid dendritic cell activation through Fc-dependent and Fc-independent mechanisms. *EMBO Mol Med* 2015;7:464–76.
62 Mora-Arias T, Amezcua-Guerra LM. Type III interferons (lambda interferons) in rheumatic autoimmune diseases. *Arch Immunol Ther Exp* 2020;68:1.
63 Suárez-Fariñas M, Ungar B, Correa da Rosa J, *et al*. RNA sequencing atopic dermatitis transcriptome profiling provides insights into novel disease mechanisms with potential therapeutic implications. *J Allergy Clin Immunol* 2015;135:1218–27.

Merola RNA Tape Sampling Manuscript Supplementary Materials

Supporting Information

Appendix 1 Supplementary materials and methods

Main inclusion criteria

To participate in this study, candidates had to meet the following eligibility criteria at the time of the day 1 visit or at the time point specified in the individual eligibility criteria listed:

1. Aged ≥ 18 years at the time of informed consent.
2. Healthy volunteers (HVs) had to be in good overall health, as determined by the investigator, based on medical history, physical examination (per standard dermatology practice) and vital signs.
3. Participants with lupus had to present with active discoid lupus erythematosus (DLE) or subacute cutaneous lupus erythematosus (SCLE) skin disease (with or without systemic manifestations of systemic lupus erythematosus [SLE], as defined by at least four out of 11 American College of Rheumatology 1997 classification criteria[1,2] for SLE).

Main exclusion criteria

Candidates were excluded from study entry if any of the following exclusion criteria existed at the time of the day 1 visit or at the time point specified in the individual criterion listed:

1. History of any clinically significant medical condition, as determined by the investigator, which could have impacted study analyses, including, but not limited to:
    a. History of HIV; history of hepatitis C virus or hepatitis B virus infection; symptoms of bacterial or viral infection (including skin infection) within 14 days before the day 1 visit; history of malignancy in the last 5 years (nonmelanoma skin cancer that was considered cured by the investigator was not exclusionary).

Merola RNA Tape Sampling Manuscript Supplementary Materials

2. Enrolment in any other drug or biologic study or treatment with an investigational drug or approved therapy for investigational use within 28 days (or five half-lives of the agent, whichever was longer) before the day 1 visit.
3. Any live or attenuated immunization or vaccination within 28 days before the day 1 visit.

Participants with DLE or SCLE were also excluded if they met any of the additional criteria:

4. Evidence of skin conditions other than DLE or SCLE at the day 1 visit that, in the opinion of the investigator, would have interfered with the study execution or analysis.
5. Change in dosage of antimalarial or systemic immunosuppressive within 28 days before the day 1 visit.
6. Treatment with prednisone at a daily oral dose > 15 mg or equivalent. Prednisone dosage must have been stable for ≥ 28 days before the day 1 visit.
7. Treatment with high-potency topical steroid and/or other topical agents (e.g. tacrolimus, pimecrolimus) to the skin lesions of interest (i.e. lesion for punch biopsy or tape harvesting) within 7 days before the day 1 visit.
8. Treatment with any of the following medications within 3 months before the day 1 visit:
    - Cyclophosphamide.
    - Any biologics (e.g. fusion proteins, therapeutic proteins or monoclonal antibodies) for SLE, including, but not limited to, belimumab or rituximab.

Study assessments

Baseline characteristics collected and analysed included medical history, including disease-specific classification criteria if applicable, patient-reported outcome (visual analogue scale pruritus), physical examinations (per standard dermatology practice), height, weight and

concomitant therapy and procedures. Additionally, the following disease-activity indices were collected and analysed: for the DLE and SCLE cohorts, Cutaneous Lupus Erythematosus Disease Area and Severity Index.[3]

Photographing of the taping site was maintained as part of the data for each participant for later validation of the transcription profile with skin manifestation.

Participants who underwent a punch biopsy on day 1 attended a follow-up visit 7 to 14 days later to have sutures removed and report procedure-related adverse events (AEs) or serious AEs. Participants who did not undergo a punch biopsy received a follow-up call 48 h after their day 1 visit.

Tape RNA extraction and quantification

A total of 30 adhesive tape sample kits were received by DermTech Inc. (La Jolla, CA, U.S.A.). Each adhesive tape sample kit contains 4 adhesive tapes strips, and 4 tape strips were used to collect each patient sample (1 kit = 4 tapes = 1 sample). Total RNA was isolated from the sample kits by placing each tape strip into a microcentrifuge tube containing 220µL of proprietary lysis solution. The lysates from 4 adhesive tape strips were pooled prior to purification with the Arcturus PicoPure RNA Isolation Kit (Life Technologies, Carlsbad, CA, U.S.A.).

Quality control for tape RNA samples is as follows. 2µL of the isolated RNA product, or a sample from a serial dilution of a known quantity of universal human reference (UHR) RNA, was added to a reverse transcription reaction (consisting of 2µL sample RNA, 5µL water, 2µL of 5x VILO Reaction Buffer and 1µL of 10X SuperScript Enzyme mix) with a final reaction volume of 10µL. The reaction was incubated at 42°C for 60 min to convert mRNA products to cDNA, from which ACTB (β-actin) gene expression products were analyzed by qPCR (with PCR primers and TaqMan probe specific to the ACTB mRNA product) on a 7900HT ABI PCR instrument. For

each sample used in the gene expression analysis, Ct values and amplification curves from qPCR for β-actin were examined and compared to those from UHR RNA. Mean sample Ct values = 25.36, SD = 2.89, indicating adequate template quality. No samples were removed from analysis due to suboptimal template quality.

Gene expression analysis and quality control

Gene expression analysis using the QuantStudio 12K Flex was a four-step process that included RNA normalization/reverse transcription, preamplification of cDNA, PCR product cleanup and qPCR gene expression quantification on TaqMan Custom OpenArray plates (for 2 custom panels of 56-genes each). Three concentrations of UHR (250, 750, and 1000pg) were used for gene expression analysis.

To convert target gene mRNA to cDNA, duplicate 96-well reverse transcription (RT) plates (1 RT plate for each gene panel) were prepared by adding 1ng of total RNA in a volume of 5μL for samples with total RNA yield ≥2 ng to the RT reaction. For samples with total RNA yields <2 ng, the RNA solution was concentrated down to ≈10μL using a Savant DNA 120 Concentrator (Thermofisher Scientific, Carlsbad CA.), and 5μL of the concentrated RNA was added to the RT reaction. Each RT reaction also included 2μL of 5x VILO Reaction Buffer and 1μL of 10x SuperScript Enzyme mix; The RT reaction plates were incubated at 42°C for 60 minutes. The 2 RT plates were prepared in parallel.

Two different custom preamplification master mixes were prepared by adding 2.5μL water, 25μL of 2X TaqMan PreAmp MasterMix, and 12.5uL of TaqMan Custom PreAmp Pool, total 40μL, for either gene panel A or gene panel B (See tables S1 and S2 for gene panels). All 40μL of the

preamp master mix for Panel A was added to cDNA wells on RT plate 1, and 40µL of the preamp master mix for Panel B were added to the cDNA wells on the RT plate 2. The 2 RT plates were returned to the thermocycler for a 16-cycle preamp reaction (95ºC for 10 min and 16 cycles of 95ºC at 15 sec and 60ºC at 4 min, then 4ºC hold). The pre-amplified cDNA products from each reaction underwent PCR cleanup using the DNA Clean and Concentrator-25 kit from Zymo Research (Irvine, CA). The cleaned PCR products cDNA were concentrated to a final volume of 9µL.

These pre-amplified and cleaned PCR products from each of the samples and 3 UHR controls for both panels A and B (Tables S1 and S2) were divided into 3 replicates of 3µL each. An equal volume (3µL) of 2X TaqMan OpenArray (OA) Realtime Master Mix was added to each sample replicate before these reaction mix solutions were transferred to 384-well OpenArray sample plates per plate maps generated with the QuantStudio 12K Flex Sample Tracker software. The 384-well OpenArray sample plates were then loaded onto the QuantStudio Accufill instrument and reaction mix from the 384-well sample plates dispensed onto the TaqMan Custom OA plates specifically for either panel A or B. The custom TaqMan OA plates were sealed and loaded onto the QS 12K Flex instrument for a 40-cycle qPCR reaction (95ºC for 20 sec and 40 cycles of 95ºC for 1 sec and 60ºC for 20 sec). A total of 6 QuantStudio Custom TaqMan OA plates were run (3 for panel A [Table S1] and 3 for panel B [Table S2]).

The quality control process for gene level expression data was as follows. Each tape-derived RNA sample was run in triplicate runs for each gene panel. The Thermo Fisher QuantStudio system supplies two quality control measures, (1) amplification score and (2) Cq confidence value, both are based on ThermoFisher developed algorithms to measure the quality of the qPCR reaction. Thresholds for these measures were set according to manufacturer

recommendations (amplification score >1.1 and Cq confidence value >0.8). The entire run for a sample replicate was omitted if more than 50% of the Ct values did not meet the acceptance criteria. Samples were also required to have acceptable data on both gene panels in order to be included in further analyses. After removal of failing replicates, the proportion of replicates not meeting these thresholds was <2%. Any Ct values greater than 25 were considered above the upper limit of quantitation and were imputed as 25. dCt values were calculated by normalizing the raw Ct values to the average of housekeeping genes within the same run. Deviation from the median was within 0.5Ct for each triplicate for the majority the data (97%) included in the final statistical analysis.

Statistics

Due to the small number of participants with DLE or SCLE, and some biomarker specimens being used up in the interim analysis (see Biomarker samples used in interim and final analyses below), no more than four participants in each disease group had both tape-derived RNA and biopsy immunohistochemistry (IHC) for the final analyses. Given 42 of the 94 total genes were measured a second time in an interim analysis for 15 tape samples (with 5 samples measured at both interim and main analysis), to increase sample size, we pooled the data from interim and final analysis for these 42 genes based on the 5 bridging samples for all statistical analysis except for the principal component and gene-cluster determination analyses.

The following strategy was used to derive log2 expression values from the raw tape-derived RNA data. Housekeeping genes were used to calibrate dCt in each replicate plate. For each sample by gene, dCt results were averaged across replicates in each batch. For each assay batch, ddCt was calibrated using the bridging samples. The ddCt results from the two batches were combined. For each gene, log2 expression (–ddCt) was calibrated to the mean of ddCt for

age-matched HVs. The missing log2 expression values were imputed using a multivariate unsupervised random forest approach.[4]

Individual samples were plotted on the first two principal components of log2 expression for all candidate genes. Using the gene expression data generated in the final analysis, candidate genes were grouped into four gene clusters based on the hierarchical clustering of the consensus of 1000 K-means results, after bootstrapping 80% of samples at each iteration (ConsensusClusterPlus R package). Using pooled data generated from interim analyses and final analyses, gene set scores and differences in gene set scores among disease groups were estimated using a linear mixed-effects model, with fixed effects for sample type and random intercepts for genes and samples. P-values from multiple comparisons were adjusted using Tukey's correction. Spearman's correlations and associated p-values were calculated to determine the associations between biomarkers from skin tape–derived RNA and IHC based on skin biopsies.

Immunohistochemistry

Tissue sections 4-µm thick were prepared. Presence of lesions was confirmed by evaluation of adjacent haematoxylin and eosin sections (data not shown). Sections were placed on charged slides, thoroughly dried, deparaffinized and rehydrated. Heat-mediated epitope retrieval was performed at 95°C using the Cell Conditioning 1 retrieval solution (pH 8; Ventana Medical Systems, Inc., Oro Valley, AZ, U.S.A.). The following antibodies were used: CD45, mouse monoclonal immunoglobulin (Ig) G1 (Abcam, Cambridge, MA, U.S.A.); CD303, mouse monoclonal IgG1 (Dendritics, Lyon, France); and myxovirus resistance protein A (MXA), mouse monoclonal IgG2a (provided by Dr. Georg Kochs, Institut fuer Virologie, Freiburg, Germany). IHC was performed using Ventana Discovery Ultra automated platform (Ventana Medical

Systems, Inc.). CD45 and CD303 antibody immunoreactivity was detected using the Ventana OmniMap-HRP detection kit, followed by incubation with Ventana Purple chromogen. MXA antibody immunoreactivity was detected using the Ventana ChromoMap-AP detection kit, followed by incubation with Ventana Red chromogen. Details are provided in table S3.

Slides were digitized with a Pannoramic P250 scanner (3DHISTECH, Budapest, Hungary) at 200× resolution and skin biopsies were hand-annotated to define epidermis and dermis. Customized image analysis algorithms were written with Visiopharm, Inc. (Hoersholm, Denmark), software using a combination of colour deconvolution and median filters. Area of immunoreactivity was quantified as percent area, with the total tissue area as the denominator.

Biomarker samples used in interim and final analyses

A 4- to 6-mm punch biopsy specimen was collected. Seventeen punch biopsy samples were obtained (eight with DLE, one with SCLE, and eight HVs) and analysed in two batches. The interim analysis included five participants with DLE and four HVs; the final analysis included five participants with DLE, one with SCLE and eight HVs. Seven participants (three with DLE and four HVs) were analysed in both batches and were used to bridge the results between the two batches.

Skin tape samples were taken according to standard DermTech, Inc., (La Jolla, CA, U.S.A.) protocols. In HVs, four tapings were collected from healthy skin, with the mastoid process the preferred site for healthy or unaffected skin. Thirty RNA samples from tape harvesting of 20 participants (nine with DLE and one with SCLE who had both affected and unaffected samples and 10 HVs with an unaffected sample) were assayed in two batches. The first batch was used to provide an interim study assessment: 15 tape-derived RNA samples from five participants with DLE and five HVs were assayed on a panel of 62 candidate genes plus five

housekeeping genes. The interim assessment also included whole blood RNA samples for 10 participants. The final batch assayed 22 (2 of the samples did not pass QC and were removed from statistical analysis) tape-derived RNA samples from 6 HVs, six with DLE, one with SCLE and on a panel of 94 candidate genes plus four housekeeping genes. Five samples had a high enough RNA yield to be conducted in both batches and were used to bridge results between the two batches. Forty-two candidate genes were included on both the interim and final panels.

Safety

The following safety information was collected: procedure-related AEs and serious AEs; haematology (haemoglobin, red blood cell count, white blood cell count and differential, platelet count and C-reactive protein); urinalysis (blood, protein, glucose and a pregnancy test for female participants); and vital signs (temperature, pulse rate and systolic and diastolic blood pressure) were assessed in all cohorts. Serology included, but was not limited to:

1. DLE and SCLE cohorts: lupus autoantibodies (antinuclear antibodies, anti–double-stranded DNA, anti-Smith, anti-ribonucleoprotein, anti-Ro/SSA, anti-La/SSB, anti-histone), complement component 3, complement component 4.
2. HV cohort: antinuclear antibodies.

Reference

1. Tan EM, Cohen AS, Fries JF, et al. The 1982 revised criteria for the classification of systemic lupus erythematosus. *Arthritis Rheum* 1982; **25**:1271–7.
2. Hochberg MC. Updating the American College of Rheumatology revised criteria for the classification of systemic lupus erythematosus. *Arthritis Rheum* 1997; **40**:1725.

3. Klein R, Moghadam-Kia S, LoMonico J *et al*. Development of the CLASI as a tool to measure disease severity and responsiveness to therapy in cutaneous lupus erythematosus. *Arch Dermatol* 2011; **147**:203–8.

4. Ishwaran H, Kogalur UB. Fast unified random forests for survival, regression, and classification (RF-SRC). R package version 2.9.1 https://rdrr.io/cran/randomForestSRC/man/rfsrc.html. [accessed Nov 20, 2019].

Merola RNA Tape Sampling Manuscript Supplementary Materials

Supporting Information

Table S1 Gene panel A

Position on chip	Gene symbol	Affy_ID	Taqman_ID	Ref Seq a(mRNA)	Gene title (name)	Amplicon length, bp
1	*STING*	224929_PM_at	Hs00736958_m1	NM_198282	Stimulator of interferon genes	56
2	*EPSTI1*	227609_PM_at	Hs01566789_m1	NM_001002264	Epithelial stromal interaction 1	59
3	*IFNG*	210354_PM_at	Hs00989291_m1	NM_000619	IFN-gamma	73
4	*BAFF*	223502_PM_s_at	Hs00198106_m1	NM_001145645	B-cell activating factor	84
5	*ISG20*	33304_PM_at	Hs00158122_m1	NM_002201	Interferon stimulated exonuclease gene 20kDa	73
6	*IFITM3*	212203_x_at	Hs03057129_s1	NM_021034	interferon induced transmembrane protein 3	105
7	*IFIT1*	203153_PM_at	Hs01911452_s1	NM_001548	Interferon-induced protein with tetratricopeptide repeats 1	156
8	*TRANK1*	213261_at	Hs00389727_m1	NM_014831	Tetratricopeptide Repeat and Ankyrin Repeat Containing	66
9	*CXCR3*	217119_PM_s_at	Hs01847760_s1	NM_001142797	Chemokine (C-X-C motif) receptor	164
10	*YWHAZ*	200640_at	Hs00852925_sH	NM_001135699.1; NM_001135701.1; NM_001135700.1; NM_001135702.1; NM_003406.3; NM_145690.2	tyrosine 3-monooxygenase/tryptophan 5-monooxygenase activation protein; zeta polypeptide	97

Merola RNA Tape Sampling Manuscript Supplementary Materials

Position on chip	Gene symbol	Affy_ID	Taqman_ID	Ref Seq a(mRNA)	Gene title (name)	Amplicon length, bp
11	*TNFSF10*	202687_PM_s_at	Hs00234356_m1	NM_001190942	Tumor necrosis factor (ligand) superfamily, member 10	61
12	*CCR7*	206337_PM_at	Hs01013469_m1	NM_001838	C-C chemokine receptor type 7	58
13	*RARRES2*	209496_PM_at	Hs00161209_g1	NM_002889	Chemerin (retinoic acid receptor responder protein 2)	114
14	*HERC5*	219863_PM_at	Hs00180943_m1	NM_016323	HECT and RLD domain containing E3 ubiquitin protein ligase 5	76
15	*UBC*	208980_s_at	Hs00824723_m1	NM_021009.5	ubiquitin C	71
16	*CLEC4C*	1555687_PM_a_at	Hs01092462_m1	NM_203503	C-type lectin domain family 4, member C (BDCA2)	72
17	*SPATS2L*	215617_at;222154_s_at;232961_at;241812_at	Hs01016364_m1	NM_001100422; NM_001100423; NM_001100424; NM_001282735; NM_001282743; NM_001282744; NM_015535	Spermatogenesis Associated, Serine-Rich 2-Like	89
18	*CCL4*	204103_PM_at	Hs00605740_g1	NM_002984	Chemokine (C-C motif) ligand 4	151
19	*TRIM56*	231876_at;214808_at;226040_at	Hs00604613_m1	NM_030961	Tripartite motif-containing protein 56	155
20	*TNF*	207113_PM_s_at	Hs00174128_m1	NM_000594	TNF-alpha	80
21	*DDX58*	222793_PM_at	Hs00204833_m1	NM_014314	DEAD (Asp-Glu-Ala-Asp) box polypeptide 58	76

Merola RNA Tape Sampling Manuscript Supplementary Materials

Position on chip	Gene symbol	Affy_ID	Taqman_ID	Ref Seq a(mRNA)	Gene title (name)	Amplicon length, bp
22	*XAF1*	206133_at	Hs01550142_m1	NM_017523; NM_199139	XIAP-associated factor 1	146
23	*IL6*	205207_PM_at	Hs99999032_m1	NM_000600	Interleukin 6	118
24	*CMKLR1*	210659_at;207652_s_at;229121_at	Hs01081979_s1	NM_001142344; NM_004072; NM_001142343; NM_001142345	Chemokine like receptor 1	73
25	*CD123/ IL3RA*	206148_at	Hs00608141_m1	NM_001267713; NM_002183	Cluster of differentiation 123	70
26	*MX1*	202086_PM_at	Hs00182073_m1	NM_001144925	Myxovirus (influenza virus) resistance 1	99
27	*IFI27*	202411_PM_at	Hs01086373_g1	NM_001130080	interferon, alpha-inducible protein 27	68
28	*OAS2*	204972_PM_at	Hs00213443_m1	NM_016817	2'-5'-oligoadenylate synthetase 2, 69/71 kDa	63
29	*IFI44*	214059_PM_at	Hs00951349_m1	NM_006417	Interferon-induced protein 44	81
30	*IL8*	202859_PM_x_at	Hs01553824_g1	NM_000584	Interleukin 8	91
31	*LY6E*	202145_PM_at	Hs03045111_g1	NM_002346	Lymphocyte antigen 6 complex, locus E	66
32	*IP10*	204533_PM_at	Hs01124251_g1	NM_001565	Interferon gamma-induced protein 10 (Chemokine [C-X-C motif] ligand 10)	135
33	*IFIT3*	204747_PM_at	Hs01922752_s1	NM_001549	Interferon-induced protein with tetratricopeptide repeats 3	137

Merola RNA Tape Sampling Manuscript Supplementary Materials

Position on chip	Gene symbol	Affy_ID	Taqman_ID	Ref Seq a(mRNA)	Gene title (name)	Amplicon length, bp
34	*B2M*	232311_at	Hs00984230_m1	NM_004048.2	beta-2-microglobulin	81
35	*CCL3*	no probe	Hs04194942_s1	NM_002983	Chemokine (C-C motif) ligand 3	95
36	*ISG15*	205483_PM_s_at	Hs01921425_s1	NM_005101	ISG15 ubiquitin-like modifier	140
37	*RTP4*	219684_PM_at	Hs00223342_m1	NM_022147	Receptor (chemosensory) transporter protein 4	58
38	*CXCL11*	210163_PM_at	Hs04187683_g1	NM_005409	Chemokine (C-X-C motif) ligand 1	113
39	*GAPDH*	AFFX-HUMGAPDH/M33197_3_at	Hs02758991_g1	NM_002046.4; NM_001256799.1	glyceraldehyde-3-phosphate dehydrogenase	93
40	*USP18*	219211_PM_at	Hs00276441_m1	NM_017414	Ubiquitin specific peptidase 18	102
41	*CMPK2*	226702_PM_at	Hs00332806_m1	NM_001256478	cytidine monophosphate (UMP-CMP) kinase 2, mitochondrial	74
42	*TCF4*	212387_at;212386_at;203753_at;213891_s_at;212385_at;228837_at;212382_at;222146_s_at	Hs00162613_m1	NM_003199; NM_001243235; NM_001083962; NM_001243234; NM_001243231; NM_001243227; NM_001243232; NM_001243233; NM_001243236; NM_001243230; NM_001243228; NM_001243226	Transcription factor (E protein) E2-2	93

Merola RNA Tape Sampling Manuscript Supplementary Materials

Position on chip	Gene symbol	Affy_ID	Taqman_ID	Ref Seq a(mRNA)	Gene title (name)	Amplicon length, bp
43	*SIGLEC1*	44673_PM_at	Hs00988063_m1	NM_023068	Sialic acid binding Ig-like lectin 1, sialoadhesin	56
44	*TRIM38*	235084_x_at;203567_s_at;238972_at;203568_s_at;203610_s_at	Hs00197164_m1	NM_006355	Tripartite Motif Containing 38	99
45	*CXCL9*	203915_PM_at	Hs00970538_m1	NM_002416	Chemokine (C-X-C motif) ligand 9	137
46	*CCL19*	210072_PM_at	Hs00171149_m1	NM_006274	Chemokine (C-C motif) ligand 19	61
47	*MOV10*	223849_s_at;233917_s_at	Hs00253093_m1	NM_020963; NM_001130079; NM_001286072	Moloney Leukemia Virus 10 Protein	86
48	*CCL5*	1555759_PM_a_at	Hs00174575_m1	NM_002985	Chemokine (C-C motif) ligand 5	63
49	*RSAD2*	213797_PM_at	Hs00369813_m1	NM_080657	Radical S-adenosyl methionine domain containing 2	76
50	*IFI44L*	204439_PM_at	Hs00915294_g1	NM_006820	Interferon-induced protein 44-like	83
51	*IRF7*	208436_PM_s_at	Hs01014809_g1	NM_001572	Interferon regulatory factor 7	77
52	*PLSCR1*	241916_PM_at	Hs01062171_m1	NM_021105	Phospholipid scramblase 1	152
53	*GALM*	235256_s_at;234974_at	Hs00373403_m1	NM_138801	Galactose Mutarotase	78
54	*IFI6*	204415_PM_at	Hs00242571_m1	NM_002038	Interferon, alpha-inducible protein 6	115
55	*OAS1*	202869_PM_at	Hs00973637_m1	NM_016816	2'-5'-oligoadenylate synthetase 1, 40/46 kDa	65

Merola RNA Tape Sampling Manuscript Supplementary Materials

Position on chip	Gene symbol	Affy_ID	Taqman_ID	Ref Seq a(mRNA)	Gene title (name)	Amplicon length, bp
56	*OAS3*	218400_PM_at	Hs00934282_g1	NM_006187	2'-5'-oligoadenylate synthetase 3, 100 kDa	189

Merola RNA Tape Sampling Manuscript Supplementary Materials

Table S2 Gene panel B

Position on chip	Gene symbol	Affy_ID	TaqMan Assay ID	Ref Seq	Gene name	Amplicon length, bp
1	ITGAM	205786_s_at	Hs01064805_m1	NM_001145808.1;NM_000632.3	integrin; alpha M (complement component 3 receptor 3 subunit)	78
2	TF	203400_s_at	Hs01067777_m1	NM_001063.3	transferrin	102
3	CD207	220428_at	Hs00210453_m1	NM_015717.3	CD207 molecule; langerin	105
4	SERPINB3	209720_s_at	Hs00199468_m1	NM_006919.2	serpin peptidase inhibitor; clade B (ovalbumin); member 3	70
5	TNFSF10	202688_at	Hs00234356_m1	NR_033994.1;NM_003810.3	tumor necrosis factor (ligand) superfamily; member 10	61
6	CD3D	213539_at	Hs00174158_m1	NM_001040651.1;NM_000732.4	CD3d molecule; delta (CD3-TCR complex)	92
7	MR1	210223_s_at	Hs01042278_m1	NM_001531.2;NM_001194999.1;NM_001195000.1	major histocompatibility complex; class I-related	78
8	MMP1	204475_at	Hs00899660_g1	NM_001145938.1;NM_002421.3	matrix metallopeptidase 1 (interstitial collagenase)	134
9	STAT1	AFFX-HUMISGF3A/M97935_3_at	Hs01013996_m1	NM_007315.3;NM_139266.2	signal transducer and activator of transcription 1; 91kDa	66
10	YWHAZ	200640_at	Hs00852925_sH	NM_001135699.1;NM_001135701.1;NM_001135700.1;NM_001135702.1;NM_003406.3;NM_145690.2	tyrosine 3-monooxygenase/tryptophan 5-monooxygenase activation protein; zeta polypeptide	97
11	GNLY	205495_s_at	Hs00246266_m1	NM_012483.2;NM_006433.3	granulysin	80
12	MS4A4A	219607_s_at	Hs01106866_m1	NM_024021.3;NM_148975.2;NM_001243266.1	membrane-spanning 4-domains; subfamily A; member 4A	92
13	OASL	205660_at	Hs00984390_m1	NM_198213.2;NM_003733.3	2'-5'-oligoadenylate synthetase-like	107
14	IL15	205992_s_at	Hs01003716_m1	NM_172175.2;NR_037840.2;NM_000585.4	interleukin 15	117
15	GAPDH	AFFX-HUMGAPDH/M33197_3_at	Hs02758991_g1	NM_002046.4;NM_001256799.1	glyceraldehyde-3-phosphate dehydrogenase	93
16	CD14	201743_at	Hs02621496_s1	NM_001040021.2;NM_000591.3;NM_001174105.1;NM_001174104.1	CD14 molecule	140

Merola RNA Tape Sampling Manuscript Supplementary Materials

Position on chip	Gene symbol	Affy_ID	TaqMan Assay ID	Ref Seq	Gene name	Amplicon length, bp
17	LILRA4	210313_at	Hs00429272_g1	NM_012276.3	leukocyte immunoglobulin-like receptor; subfamily A (with TM domain); member 4	76
18	S100A9	203535_at	Hs00610058_m1	NM_002965.3	S100 calcium binding protein A9	83
19	CD86	205686_s_at	Hs01567026_m1	NM_175862.4;NM_001206925.1;NM_006889.4;NM_176892.1;NM_001206924.1	CD86 molecule	104
20	CD8A	205758_at	Hs00233520_m1	NM_001768.6;NR_027353.1;NM_171827.3;NM_001145873.1	CD8a molecule	58
21	CXCL13	205242_at	Hs00757930_m1	NM_006419.2	chemokine (C-X-C motif) ligand 13	70
22	KLRK1	205821_at	Hs00183683_m1	NM_007360.3	KLRC4-KLRK1 readthrough;killer cell lectin-like receptor subfamily K; member 1	85
23	CD69	209795_at	Hs00156399_m1	NM_001781.2	CD69 molecule	94
24	AIM2	206513_at	Hs00915711_m1	NM_004833.1	absent in melanoma 2	142
25	GZMB	210164_at	Hs00188051_m1	NM_004131.4	granzyme B (granzyme 2; cytotoxic T-lymphocyte-associated serine esterase 1)	114
26	VCAM1	203868_s_at	Hs00365486_m1	NM_001199834.1;NM_080682.2;NM_001078.3	vascular cell adhesion molecule 1	122
27	IL1B	39402_at	Hs01555413_m1	NM_000576.2	interleukin 1; beta	136
28	IL24	206569_at	Hs01114274_m1	NM_001185156.1;NM_001185157.1;NM_006850.3;NM_001185158.1	interleukin 24	67
29	IL10RA	204912_at	Hs00155485_m1	NM_001558.3;NR_026691.1	interleukin 10 receptor; alpha	72
30	CASP1	211368_s_at	Hs00354836_m1	NM_033292.3;NM_033293.3;NM_033294.3;NM_033295.3;NM_001257118.1;NM_001223.4;NM_001257119.1	caspase 1; apoptosis-related cysteine peptidase	76
31	IL22	222974_at	Hs00220924_m1	NM_020525.4	interleukin 22	68
32	IL13	207844_at	Hs01124272_g1	NM_002188.2	interleukin 13	73
33	S100A7	205916_at	Hs00161488_m1	NM_002963.3	S100 calcium binding protein A7	105
34	UBC	208980_s_at	Hs00824723_m1	NM_021009.5	ubiquitin C	71
35	IGJ	212592_at	Hs00950678_g1	NM_144646.3	immunoglobulin J polypeptide; linker protein for immunoglobulin alpha and mu polypeptides	85
36	ICAM1	202638_s_at	Hs99999152_m1	NM_000201.2	intercellular adhesion molecule 1	99

Merola RNA Tape Sampling Manuscript Supplementary Materials

Position on chip	Gene symbol	Affy_ID	TaqMan Assay ID	Ref Seq	Gene name	Amplicon length, bp
37	IL9	208193_at	Hs00914237_m1	NM_000590.1	interleukin 9	104
38	CD163	203645_s_at	Hs01016662_m1	NM_004244.5;NM_203416.3	CD163 molecule	87
39	B2M	232311_at	Hs00984230_m1	NM_004048.2	beta-2-microglobulin	81
40	TRGV9	209813_x_at	Hs01379483_g1		T cell receptor gamma variable 9	72
41	SERPINB4	211906_s_at	Hs01691254_g1		serpin peptidase inhibitor; clade B (ovalbumin); member 4	156
42	HESX1	211267_at	Hs00172696_m1	NM_003865.2	HESX homeobox 1	110
43	KLRF1	220646_s_at	Hs00212979_m1	NM_016523.1	killer cell lectin-like receptor subfamily F; member 1	70
44	CD19	206398_s_at	Hs01047409_g1	NM_001178098.1;NM_001770.5	CD19 molecule	88
45	KLRD1	210606_x_at	Hs00233844_m1	NM_002262.3;NM_001114396.1;NM_007334.2	killer cell lectin-like receptor subfamily D; member 1	100
46	IL7R	205798_at	Hs00902338_g1	NM_002185.3	interleukin 7 receptor	89
47	PRF1	214617_at	Hs00169473_m1	NM_005041.4;NM_001083116.1	perforin 1 (pore forming protein)	106
48	MS4A1	210356_x_at	Hs00544819_m1	NM_152866.2;NM_021950.3	membrane-spanning 4-domains; subfamily A; member 1	123
49	CD83	204440_at	Hs01077170_g1	NM_004233.3;NM_001251901.1	CD83 molecule	126
50	CXCL10	204533_at	Hs01124252_g1	NM_001565.3	chemokine (C-X-C motif) ligand 10	83
51	S100A8	202917_s_at	Hs00374264_g1	NM_002964.4	S100 calcium binding protein A8	107
52	KRT6A	209125_at	Hs01699178_g1	NM_005554.3	keratin 6A	83
53	HLA-DRB1	208306_x_at	Hs03027795_uH	NM_021983.4	major histocompatibility complex; class II; DR beta 4	131
54	FAS	204781_s_at	Hs00907759_m1	NR_028033.2;NR_028035.2;NM_000043.4;NM_152871.2;NR_028034.2;NR_028036.2	Fas cell surface death receptor	118
55	CCL2	216598_s_at	Hs00234140_m1	NM_002982.3	chemokine (C-C motif) ligand 2	101
56	ITGAX	210184_at	Hs01015070_m1	NM_000887.3	integrin; alpha X (complement component 3 receptor 4 subunit)	69

Merola RNA Tape Sampling Manuscript Supplementary Materials

Table S3 Detailed immunohistochemistry methods

Marker	Antigen retrieval	Antibody final concentration or dilution	Antibody incubation time and temperature	Ventana pre-treatment kit used	Ventana secondary detection kit used	Chromogen	Autostainer platform used
CD45	CC1, 64 min at 93°C	0.5 µg/mL	60 min, ambient T°C	Chromo-HRP Map kit	Omni Mouse-HRP	Ventana Purple	Ventana Ultra
CD303	CC1, 64 min at 93°C	20 µg/mL	1 h, 36 °C	Chromo-HRP Map kit	Omni Mouse-HRP	Ventana Purple	Ventana Ultra
MXA-1	CC1, 60 min at 95 °C	1:3500 dilution of the stock	60 min, ambient T°C	Chromo Red kit	Ultra Mouse-AP	Ventana Red	Ventana XT

Merola RNA Tape Sampling Manuscript Supplementary Materials

Table S4 Biopsy sites

Participant number	**Biopsy site**
Cutaneous lupus erythematosus[a]	
1	Left eyebrow
2	Left temple
3	Vertex, scalp
4	Left shoulder/upper back
7	Left posterior scalp
13	Scalp
21	NA[b]
22	Center of posterior shoulders
23	Left scalp
24 (subacute cutaneous lupus erythematosus)	Left, mid back just below bra line
Healthy volunteers	
5	Left upper extremity
6	Right upper extremity
8	Left arm (medially, near axilla)
9	Right inner upper arm
10	Right inner upper extremity
11	Right upper inner arm
12	Right flank
15	Inner right upper arm
17	Upper right arm
18	Right forearm

NA, not applicable.
[a]All participants had discoid lupus erythematosus except where indicated. [b]Biopsy sample is missing.

Merola RNA Tape Sampling Manuscript Supplementary Materials

Table S5 Morphologic descriptions of biopsied samples

Diagnosis	Subject Number	Interface dermatitis	Acanthosis, hyperkeratosis or other epidermal changes	Perivascular dermatitis	Periadnexal dermatitis	Cumulative Score	Additional features
DLE	1	2	2	1	2	7	Moderate interface dermatitis with segmental epidermal and papillary dermal necrosis, and multifocal coccoid bacteria in overlying serocellular crust
DLE	2	1	1	2	2	6	Moderate numbers of intraepithelial CD45+ round cells
DLE	3	2	2	2	2	8	Liquefactive necrosis of papillary dermis, epidermal and follicular acanthosis, orthokeratotic epidermal hyperkeratosis, moderate numbers of intraepithelial CD45+ round cells
DLE	4	3	1	3	2	9	Vacuolar interface dermatitis with multifocal dyskeratosis and moderate CD45+ inflammatory cell infiltration into stratum spinosum
DLE	7	3	3	2	2	10	Severe epidermal and follicular parakeratotic hyperkeratosis with follicular plugging; prominent deep dermal perivascular lymphocytic infiltrate
DLE	13	n/a	n/a	n/a	n/a	n/a	Block missing
DLE	22	n/a	n/a	3	2	n/a	Epidermis missing from block (separated during processing). Presence of multifocal small mononuclear cells at the dermal/epidermal junction with basement membrane thickening suggests detached epidermis is secondary to prominent interface dermatitis

Merola RNA Tape Sampling Manuscript Supplementary Materials

Diagnosis	Subject Number	Interface dermatitis	Acanthosis, hyperkeratosis or other epidermal changes	Perivascular dermatitis	Periadnexal dermatitis	Cumulative Score	Additional features
DLE	23	3	2	3	3	11	Prominent basement membrane thickening, follicular plugging with associated moderate epidermal and follicular hyperkeratosis and acanthosis, and prominent interface dermatitis involving follicles and deep perivascular lymphocytic/mononuclear cell infiltrate
SCLE	24	1	0	1	1	3	Interface dermatitis mild and focal with a moderate amount of CD45+ intraepithelial lymphocytes

Morphologic scores from examination of H&E and anti-CD45 reacted tissue sections from biopsy of affected sites.
Scale: 0, none; 1, mild, focal to multifocal; 2, moderate, multifocal; 3, severe, regionally extensive. Colors correlate with score. Features are grouped under one scale while cumulative score is colored according to a separate scale
DLE, discoid lupus erythematosus, SCLE, subacute lupus erythematosus

Merola RNA Tape Sampling Manuscript Supplementary Materials

Table S6 Removed genes

Removed genes
IL9, *IL24*, *IL13*, *IL22*,
TRGV9, CD10, *MS4A1*, *TNFSF10*

Merola RNA Tape Sampling Manuscript Supplementary Materials

Table S7 Candidate genes by cluster

Cluster 1 (CLE cluster)	Cluster 2 (CLE2 cluster)	Cluster 3 (IFN cluster)	Cluster 4
BAFF	*PLSCR1*	*IFI44L*	*HLA-DRB1*
ITGAX	*HERC5*	*IFI27*	*KRT6A*
ISG15	*STAT1*	*IFI6*	*S100A7*
CCL2	*PRF1*	*OAS1*	*S100A9*
CD163	*TRANK1*	*OAS2*	*CD14*
IP10	*LY6E*	*OAS3*	*CCL3*
CXCL13	*ISG20*	*RSAD2*	*CXCR3*
GZMB	*KLRD1*	*CCL5*	*CMKLR1*
TNF	*SPATS2L*	*CXCL9*	*LILRA4*
IL1B	*MR1*	*GNLY*	
SERPINB4	*TF*	*OASL*	
IL6	*GALM*	*CMPK2*	
SERPINB3	*IFITM3*	*EPSTI1*	
IFIT3	*MOV10*	*MX1*	
IL8	*TRIM38*	*SIGLEC1*	
CCL4	*TRIM56*	*USP18*	
IFIT1	*HESX1*	*IFI44*	
MMP1	*KLRF1*	*XAF1*	
ICAM1	*CLEC4C*		
MS4A4A	*IFNG*		

Merola RNA Tape Sampling Manuscript Supplementary Materials

Cluster 1 (CLE cluster)	Cluster 2 (CLE2 cluster)	Cluster 3 (IFN cluster)	Cluster 4
CXCL11	*RARRES2*		
CD69	*STING*		
CD86	*CD207*		
IL7R	*TCF4*		
CD83	*CASP1*		
CD8A	*CD3D*		
IL10RA	*IRF7*		
KLRK1	*VCAM1*		
CD123/IL3RA	*DDX58*		
CCR7	*FAS*		
IGJ	*IL15*		
	RTP4		

Gene lists of the four gene clusters obtained from consensus of K-mean clustering algorithm. *AIM2*, *S100A8*, *ITGAM*, and *CCL19* were not consistently grouped with any of the four clusters and were removed from the table. Cluster 1: CLE cluster. Cluster 2: CLE2 cluster. Cluster 3: IFN cluster. CLE, cutaneous lupus erythematosus; IFN, interferon.

Merola RNA Tape Sampling Manuscript Supplementary Materials

Table S8 Comparisons of cutaneous lupus erythematosus-affected, cutaneous lupus erythematosus-unaffected and healthy volunteer skin samples by gene cluster

	Cluster 1		Cluster 2		Cluster 3		Cluster 4	
Comparison	fc	p	fc	p	fc	P	fc	p
CLE-A vs. HV-U	4.11	0.005	2.67	0.001	23.25	<0.001	1.13	0.963
CLE-U vs. HV-U	1.15	0.95	1.45	0.388	3.08	0.139	0.71	0.766
CLE-A vs. CLE-U	3.59	0.012	1.84	0.077	7.54	0.002	1.59	0.598

CLE-A, cutaneous lupus erythematosus-affected skin; CLE-U, cutaneous lupus erythematosus-unaffected skin; fc, fold change; p, p-value; HV-U, healthy volunteer-unaffected skin.

Merola RNA Tape Sampling Manuscript Supplementary Materials

Table S9 Ingenuity pathway analysis of gene clusters

Ingenuity canonical pathways	–log(p-value)	Molecules
CLE-associated cluster (1)		
Communication between innate and adaptive immune cells	16.3	*CCL4*, *CCR7*, *CD83*, *CD86*, *CD8A*, *CXCL10*, *CXCL8*, *IL1B*, *IL6*, *TNF*, *TNFSF13B*
TREM1 signalling	13.4	*CCL2*, *CD83*, *CD86*, *CXCL8*, *ICAM1*, *IL1B*, *IL6*, *ITGAX*, *TNF*
Role of hypercytokinemia/ hyperchemokinemia in the pathogenesis of influenza	13	*CCL2*, *CCL4*, *CXCL10*, *CXCL8*, *IFIT3* ,*IL1B* ,*IL6*, *ISG15*, *TNF*
Granulocyte adhesion and diapedesis	12.1	*CCL2*, *CCL4*, *CXCL10*, *CXCL11*, *CXCL13*, *CXCL8*, *ICAM1*, *IL1B*, *MMP1*, *TNF*
IFN-dominant cluster (3)		
Role of hypercytokinemia/ hyperchemokinemia in the pathogenesis of influenza	8.9	*CCL5*, *MX1*, *OAS1*, *OAS2*, *OAS3*, *RSAD2*
Interferon signalling	4.4	*IFI6*, *MX1*, *OAS1*
Role of pattern recognition receptors in recognition of bacteria and viruses	4.3	*CCL5*, *OAS1*, *OAS2*, *OAS3*
Pathogenesis of multiple sclerosis	3.8	*CCL5*, *CXCL9*

Ingenuity pathway analysis on two clusters reveals overlap with genes classically associated with immune-mediated pathogenesis in lupus erythematosus. The top 4 enriched pathways are shown for each cluster, ranked by -log(p-value) after correction for multiple comparisons. CLE, cutaneous lupus erythematosus, IFN, interferon.

Merola RNA Tape Sampling Manuscript Supplementary Materials

Table S10 Twenty-two–gene INF signature

Included genes based on whole blood
CMPK2, *DDX58*, *EPSTI1*, *HERC5*, *IFI27*, *IFI44*, *IFI6*, *IFIT1*, *IFIT3*, *ISG15*, *LAMP3*, *LIPA*, *LY6E*, *MX1*, *OAS1*, *OAS3*, *PLSCR1*, *RSAD2*, *RTP4*, *TIMM10*, *UBE2L6*, *USP18*

Merola RNA Tape Sampling Manuscript Supplementary Materials

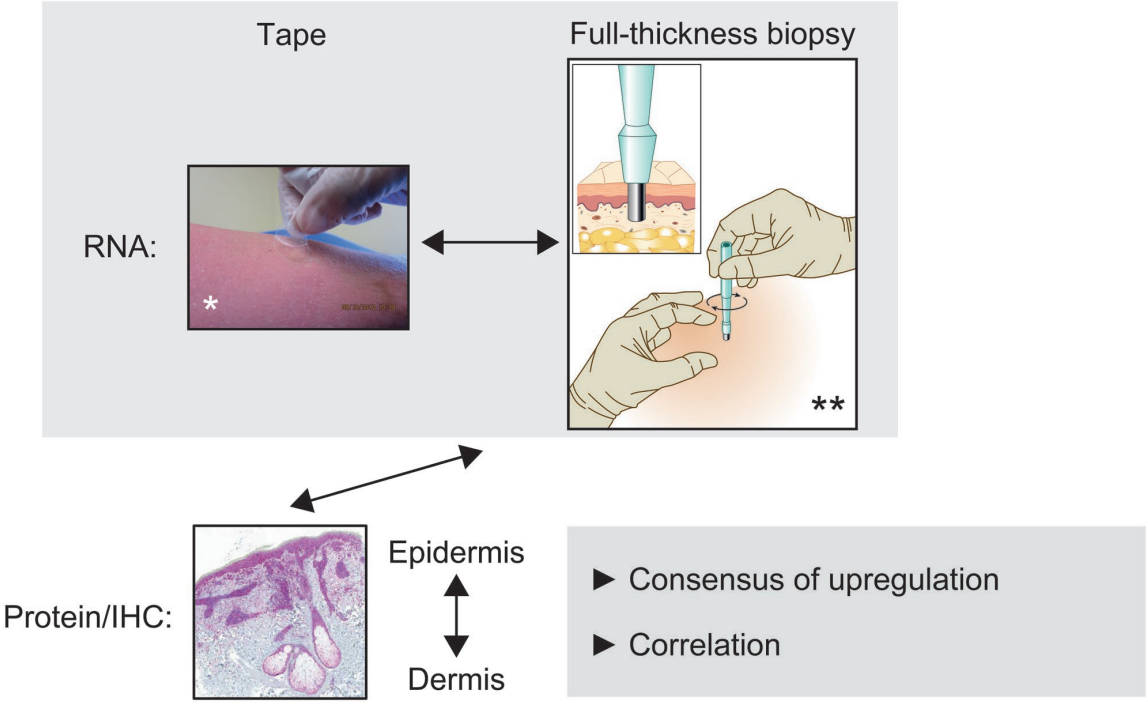

Figure S1 Schematic of study goals. This cross-sectional study compared a non-invasive method (collection of RNA from the skin surface using a tape device) with a relatively invasive method (full-thickness tissue biopsy). RNA from candidate genes was compared with hallmark proteins for consensus of upregulation and for correlation. IHC, immunohistochemistry. *Photograph courtesy of DermTech, Inc. (La Jolla, CA, U.S.A.). **Used with permission of Mayo Foundation for Medical Education and Research, all rights reserved.

Merola RNA Tape Sampling Manuscript Supplementary Materials

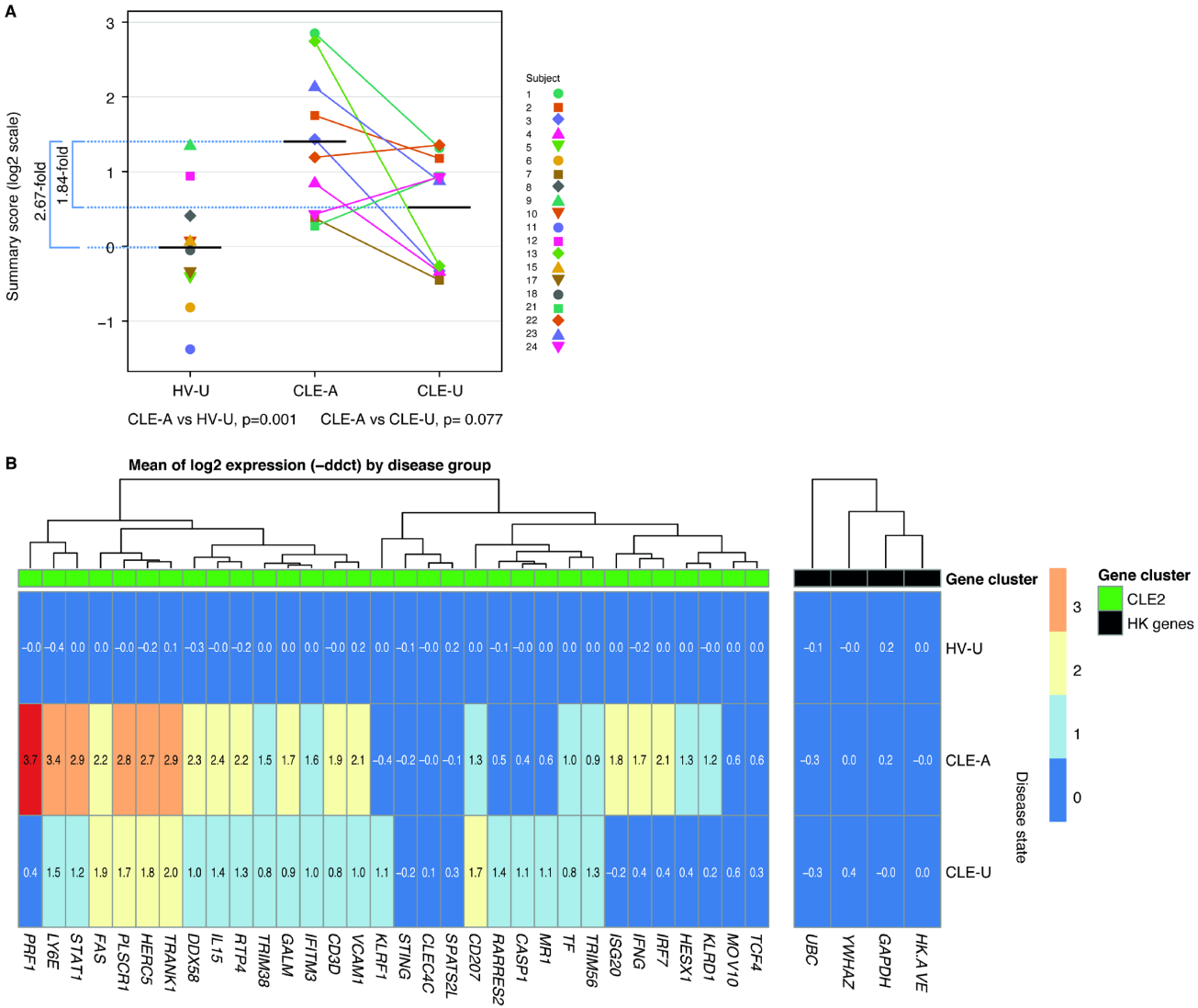

Merola RNA Tape Sampling Manuscript Supplementary Materials

Figure S2. Summary scores for the cutaneous lupus erythematosus (CLE2)–associated gene cluster differentiate healthy volunteers from the CLE-A group and heat map of cutaneous lupus erythematosus (CLE2)–associated gene expression by disease group. (A) Gene expression in CLE-affected skin, CLE-unaffected skin, and healthy volunteers for the CLE2-associated gene cluster (cluster 2). (B) Log2 fold change from the mean of healthy volunteers (HV) for each gene in CLE2-associated cluster. Log2 fold change for 3 housekeeping (HK) genes (*GAPDH*, *UBC*, *YWHAZ*), and the average log2 fold change for these three HK genes (HK.AVE), are shown (black boxes in top row). Log2 fold changes are given by colour (red, increased; dark blue, decreased) and by value in each cell. Relatedness of gene expression log2 fold changes is depicted with a dendrogram across the top of the figure. Disease groups are listed along the y-axis. Genes are listed along the x-axis. CLE-A, cutaneous lupus erythematosus-affected skin; CLE-U, cutaneous lupus erythematosus-unaffected skin; HV-U, healthy volunteer-unaffected skin

Merola RNA Tape Sampling Manuscript Supplementary Materials

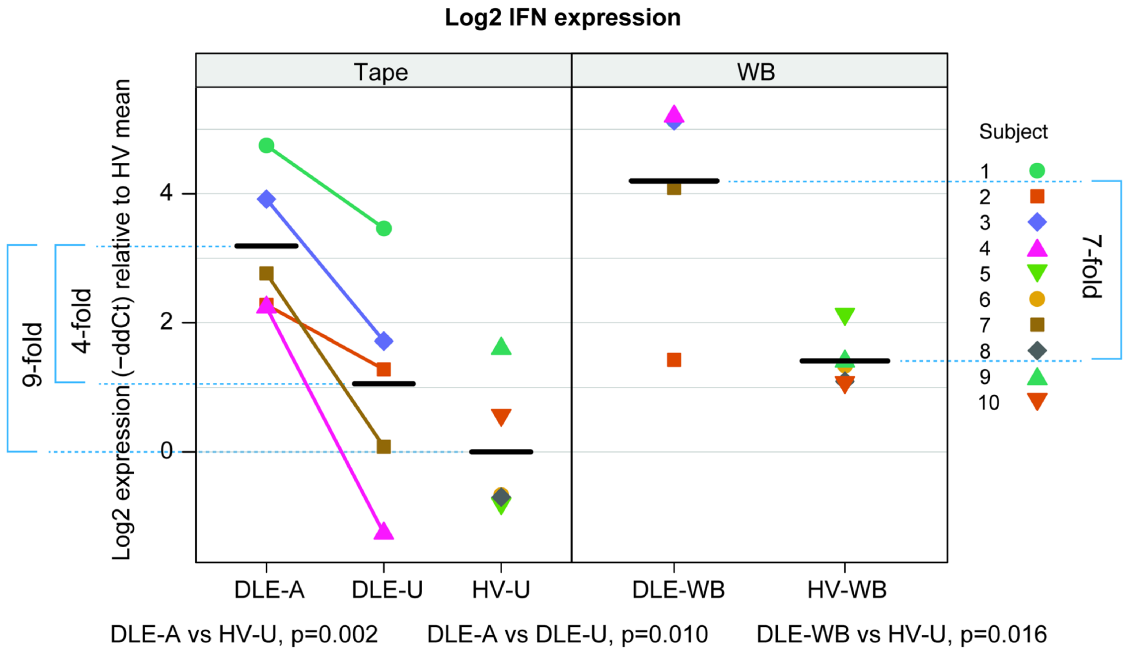

Figure S3 Differential expression of interferon (IFN) genes is more pronounced in skin tape than whole blood samples. Detection of a 22-gene IFN-I signature expression in skin with the DermTech, Inc. (La Jolla, CA, U.S.A.), tape device compared with the same genes in whole blood. Each coloured symbol stands for a single participant. For the purposes of calibration, the mean HV dCt was set at 0 by subtracting the mean HV dCt from all datapoints. DLE-A, discoid lupus erythematosus-affected skin; DLE-U, discoid lupus

erythematosus-unaffected skin, DLE-WB, discoid lupus erythematosus-whole blood; HV-U, healthy volunteer unaffected skin; HV-WB, healthy volunteer-whole blood.

Merola RNA Tape Sampling Manuscript Supplementary Materials

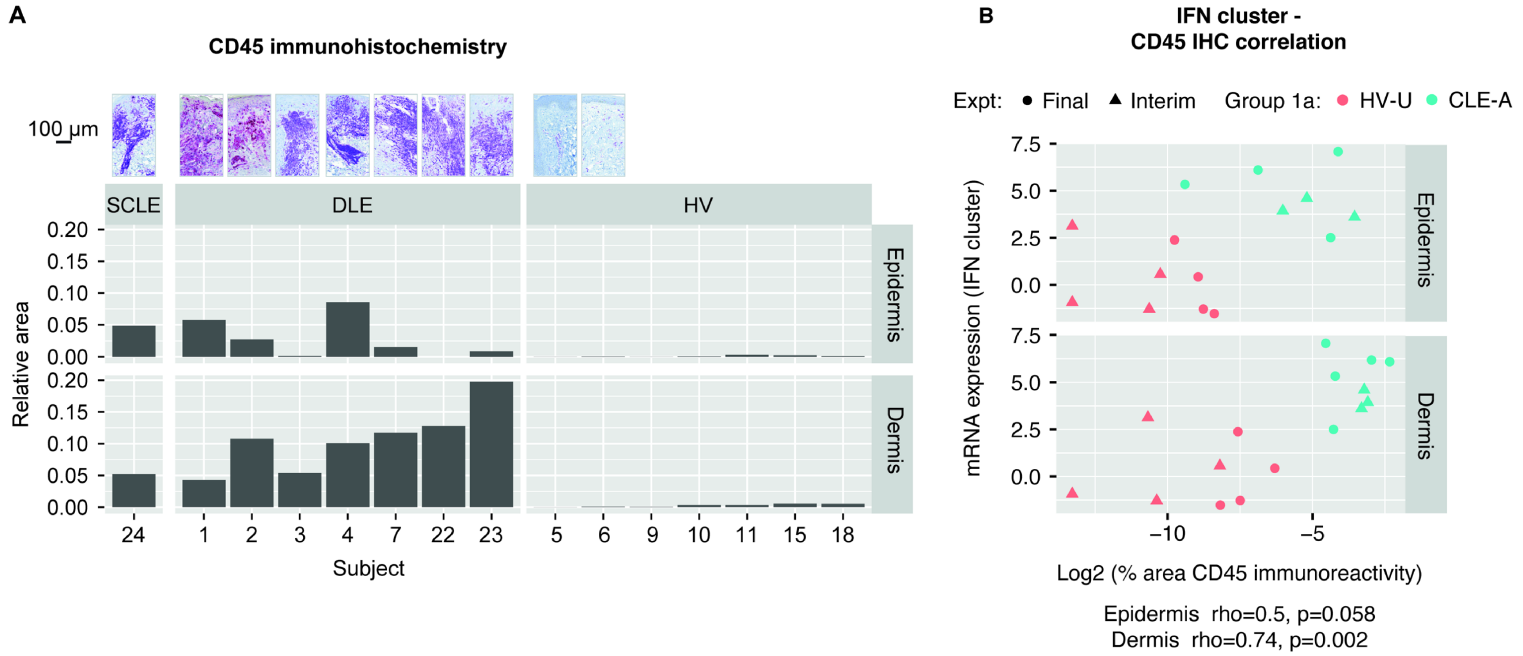

Figure S4 (A) CD45 immunohistochemistry and (B) CD45 immunohistochemistry (IHC) interferon (IFN) gene cluster correlation. CLE, cutaneous lupus erythematosus; CLE-A, cutaneous lupus erythematosus-affected skin; DLE, discoid lupus erythematosus; Expt, experiment; HV, healthy volunteer; HV-U, healthy volunteer-unaffected skin; mRNA, messenger RNA; SCLE, subacute cutaneous lupus erythematosus.

Merola RNA Tape Sampling Manuscript Supplementary Materials

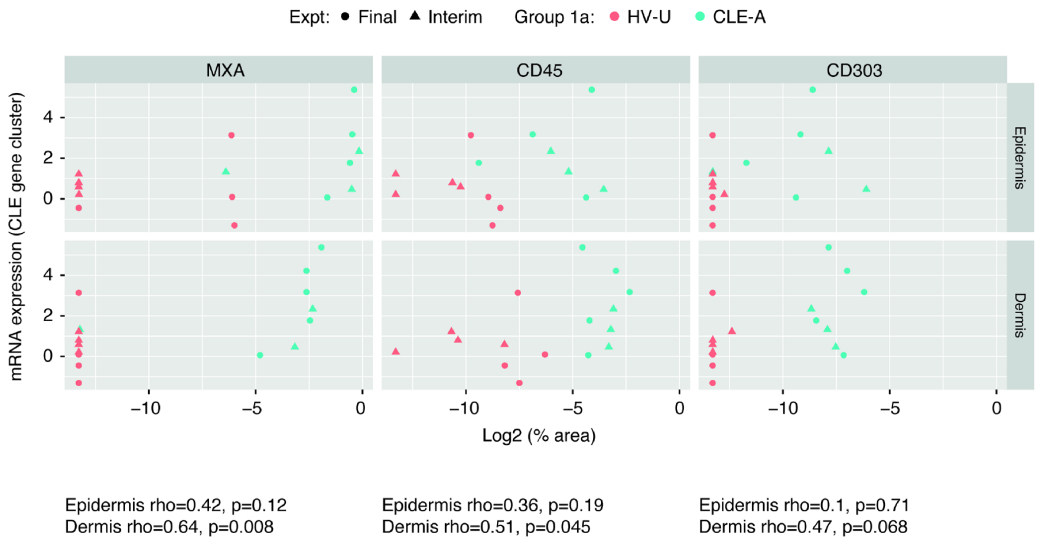

Figure S5 Cutaneous lupus erythematosus (CLE-associated) gene cluster immunohistochemistry correlation plots. CLE-A, cutaneous lupus erythematosus-affected skin; Expt, experiment; HV, healthy volunteer; mRNA, messenger RNA; MXA, myxovirus resistance protein A; HV-U, healthy volunteer-unaffected skin.